PLOS PATHOGENS

RESEARCH ARTICLE

Inhibition of polo-like kinase 1 (PLK1) facilitates reactivation of gamma-herpesviruses and their elimination

Ayan Biswas[1,2☯], **Dawei Zhou**[1☯], **Guillaume N. Fiches**[1], **Zhenyu Wu**[1,3], **Xuefeng Liu**[1,4], **Qin Ma**[3], **Weiqiang Zhao**[1], **Jian Zhu**[1]*, **Netty G. Santoso**[1]*

1 Department of Pathology, Ohio State University College of Medicine, Columbus, Ohio, United States of America, **2** Department of Genetics, School of Medicine, Unversity of Alabama at Birmingham, Birmingham, Alabama, United States of America, **3** Department of Biomedical Informatics, Ohio State University College of Medicine, Columbus, Ohio, United States of America, **4** Department of Pathology, Center for Cell Reprogramming, Georgetown University Medical Center, Washington, D.C., United States of America

☯ These authors contributed equally to this work.
* Jian.Zhu@osumc.edu (JZ); Netty.Santoso@osumc.edu (NGS)

Citation: Biswas A, Zhou D, Fiches GN, Wu Z, Liu X, Ma Q, et al. (2021) Inhibition of polo-like kinase 1 (PLK1) facilitates reactivation of gamma-herpesviruses and their elimination. PLoS Pathog 17(7): e1009764. https://doi.org/10.1371/journal.ppat.1009764

Editor: Shou-Jiang Gao, UPMC Hillman Cancer Center, UNITED STATES

Received: March 22, 2021

Accepted: June 29, 2021

Published: July 23, 2021

Data Availability Statement: All relevant data are within the manuscript and its Supporting information files.

Funding: This work was supported by grants to NGS [R03DE029716, R01CA260690] and JZ [R01DE025447, R01AI150448, R33AI116180] from the National Institute of Health (https://www.nih.gov). The funders had no role in study design, data collection and analysis, decision to publish, or preparation of the manuscript.

Abstract

Both Kaposi's sarcoma-associated herpesvirus (KSHV) and Epstein-Barr virus (EBV) establish the persistent, life-long infection primarily at the latent status, and associate with certain types of tumors, such as B cell lymphomas, especially in immuno-compromised individuals including people living with HIV (PLWH). Lytic reactivation of these viruses can be employed to kill tumor cells harboring latently infected viral episomes through the viral cytopathic effects and the subsequent antiviral immune responses. In this study, we identified that polo-like kinase 1 (PLK1) is induced by KSHV *de novo* infection as well as lytic switch from KSHV latency. We further demonstrated that PLK1 depletion or inhibition facilitates KSHV reactivation and promotes cell death of KSHV-infected lymphoma cells. Mechanistically, PLK1 regulates Myc that is critical to both maintenance of KSHV latency and support of cell survival, and preferentially affects the level of H3K27me3 inactive mark both globally and at certain loci of KSHV viral episomes. Furthremore, we recognized that PLK1 inhibition synergizes with STAT3 inhibition to efficiently induce KSHV reactivation. We also confirmed that PLK1 depletion or inhibition yields the similar effect on EBV lytic reactivation and cell death of EBV-infected lymphoma cells. Lastly, we noticed that PLK1 in B cells is elevated in the context of HIV infection and caused by HIV Nef protein to favor KSHV/EBV latency.

Author summary

KSHV is a large double-stranded DNA virus belonging to human gamma-herpesviruses and capable of establishing the long-term persistent infection, which causes cancers under immunocompromised states, such as acquired immunodeficiency syndrome (AIDS). There are currently still no effective therapies to specifically treat KSHV-associated tumors, nor eliminate its persistent infection. In this study, we illustrated that PLK1 is upregulated by KSHV, which in return suppresses KSHV lytic infection. We further

Competing interests: The authors have declared that no competing interests exist.

demonstrated that PLK1 is a novel host target that can be inhibited pharmacologically to benefit the viral oncolysis for promotion of KSHV lytic reactivation and elimination of KSHV-positive lymphoma cells, particularly for people living with HIV (PLWH). PLK1 inhibitors also exerted the similar effect on EBV that is the other member of human gamma-herpesvirus.

Introduction

Kaposi's sarcoma-associated herpesvirus (KSHV), is an etiological agent of Kaposi's sarcoma (KS)–a common AIDS-associated malignancy [1], as well as two lymphoproliferative diseases, namely primary effusion lymphoma (PEL) and multicentric Castleman's disease (CAD) [2]. KSHV has a diverse range of *in vivo* and *in vitro* cell tropism, but CD19+ B cells appear to be the primary cell type of KSHV persistent infection [3,4]. Similar to other herpesviruses, KSHV infection also includes latent and lytic phases [5,6]. Following acute infection, KSHV establishes latency in most of immunocompetent individuals, primarily in B cells [6]. Such KSHV latently infected B cells constitute a major source of KSHV viral reservoirs to maintain KSHV genomes and propagate new KSHV viruses. At the latent phase, only a limited subset of KSHV latent genes are expressed, while most of lytic genes are silenced to escape from the host immune surveillance. Latent KSHV can be reactivated in response to certain stimuli, and expression of viral lytic genes is turned on to produce new virions during viral lytic cycle. Epstein-barr virus (EBV) belongs to the same human γ-herpesvirus family as KSHV, and also primarily infect B cells in a latent phase that can be reversed to lytic replication. It is interesting to note that nearly 70% of PEL cell lines are co-infected with EBV. Studies have demonstrated that EBV co-infected PEL cell lines are more tumorigenic compared to the EBV negative ones [7].

Oncolytic viruses have been recently engineered as novel anticancer agents and shown to increase the therapeutic promise [8]. Similarly, lytic reactivation of intrinsic latent viruses, such as human endogenous retroviruses (HERVs), in tumor cells can also lead to oncolysis and therefore can be applied as an anticancer therapy [9]. The same approach has been applied for elimination of KSHV-infected tumor cells through viral oncolysis. Agonists or antagonists modulating certain cell signaling have been employed to reactivate latent KSHV, which are successful in eliminating KSHV-infected tumor cells [10]. This is mostly due to the virus-induced cytopathic effect that promotes the death of virus-reactivated cell. Although these findings are promising, such approach is still at infancy and have received only limited investigation so far. Therefore, we are interested in understanding the common cellular mechanisms associated with not only reactivation of latent KSHV and EBV but also cell survival of KSHV/EBV-reactivated tumor cells, which can be employed as a therapeutic strategy to eliminate the tumor cells harboring these oncoviruses.

PLK1 is the member of the serine/threonine polo-like kinase (PLK) family (PLK 1–4), which are key players of multiple cellular functions, including cell cycle progression, cellular stress response, and innate immune signaling [11–13]. Additionally, PLK1 was shown to regulate cell survival through stabilization of Myc protein in various tumors including B-cell lymphomas [14]. PLK1 expression is often elevated in various human cancers, and links to tumor aggressiveness and poor clinical prognosis. Recently, we reported that PLK1 protein is elevated due to HIV infection of $CD4^+$ T cells that contributes to cell survival [15]. However, there is currently no report regarding PLK1's role in the regulation of viral infection and oncogenesis of human gamma-herpesviruses. In this study, we directly address PLK1's role in KSHV

infection. We identified that PLK1 expression was induced by KSHV viral infection and played a critical role in maintaining latent infection of KSHV in B lymphoma cells as well as supporting their cell survival status via Myc protein. We further showed that specific inhibition of PLK1 facilitated viral lytic reactivation of KSHV and elimination of B lymphoma cells harboring KSHV episomes. We also observed similar functions of PLK1 in EBV-infected B lymphoma cells. PLK1 inhibitors are demonstrated to have promising results to inhibit cell survival of tumor cells *vs* non-tumor cells [16], and our study suggests that they can be further considered for viral oncolysis approach to treat KSHV/EBV-positive B lymphomas particularly in PLWH, based on the result that PLK1 expression in B cells was also induced in the setting of HIV co-infection.

Results

PLK1 is induced by KSHV infection and required for KSHV latency

We first determined the impact of KSHV infection on PLK1 expression. SLK cells, a renal carcinoma cell line with epithelial-cell origin, were spinoculated with KSHV.BAC16 viruses. KSHV infection rate was quantified by measuring the GFP expression from KSHV viral genomes in the infected cells. Fluorescence imaging showed that KSHV *de novo* infection significantly induced the expression of PLK1 protein by the immunofluorescence assays (IFAs) in SLK cells at 24hpi (Fig 1A). Similarly, we observed the PLK1 upregulation in the telomerase-immortalized human microvascular endothelial (TIME) cells *de novo* infected with KSHV.BAC16 (S1A and S1B Fig). We also evaluated PLK1 protein expression upon KSHV lytic switch from latency. iSLK.BAC16 cells [17] were treated with either Dox (doxycycline) to induce KSHV RTA expression and consequently lytic reactivation, or vehicle control to keep KSHV at latency. Fluorescence imaging confirmed that KSHV lytic reactivation also significantly induced expression of PLK1 protein by IFAs in iSLK.BAC16 cells (Fig 1B), whereas Dox treatment had no effect on PLK1 protein expression in SLK cells.

To investigate the role of PLK1 in regulating KSHV infection, we used siRNAs targeting PLK1 (siPLK1) through transient transfection for PLK1 knockdown, while non-target siRNA (siNT) was used as a control. We tested two siRNAs targeting PLK1, siPLK1-1, 2, which led to the efficient PLK1 knockdown while causing miminal cytotoxicity in KSHV-negative SLK cells (S1C Fig). We further transfected these siRNAs in BCBL1 cells, a PEL cell line latently infected with KSHV, which also efficiently depleted PLK1 (S1D Fig), while further enhancing KSHV lytic reactivation in BCBL1 cells treated with 12-O-tetra-decanoylphorbol-13-acetate (TPA) and sodium butyrate (TPA/NaB) but not at the un-treated condition through measurement of KSHV viral DNA copy number in supernatants (S1E Fig). siPLK1-2 (as siPLK1) showed the better effect of KSHV lytic reactivation, which was used for latter assays. Next, we depleted expression of endogenous PLK1 in TREx BCBL-Rta cells using siPLK1. PLK1 depletion led to a slight reduction of cell viability, especially in Dox-treated, i.e. KSHV-reactivated, cells (Fig 1C). siPLK1 knockdown efficiency was confirmed by immunoblotting of PLK1 protein in these cells (Fig 1D). Meanwhile, we noticed that PLK1 depletion significantly increased KSHV lytic reactivation specifically in Dox-treated cells but not the un-treated ones through measurement of K8.1 lytic protein by immunoblotting (Fig 1D). We observed similar effects of siRNA-mediated PLK1 depletion (Fig 1F) on KSHV lytic switch in iSLK.r219 cells through measurement of RFP expression from KSHV lytic PAN promoter by fluorescent imaging (Fig 1E) or KSHV lytic gene expression (ORF26, K8) by RT-qPCR (Fig 1F). These results indicate that the presence of PLK1 protein was necessary but not sufficient for maintenance of KSHV latency. Alternatively, we also confirmed such function of PLK1 by gain-of-function analysis. A pLEX vector expressing V5-tagged PLK1 (pLEX-PLK1) or FLAG peptide (pLEX-FLAG) was

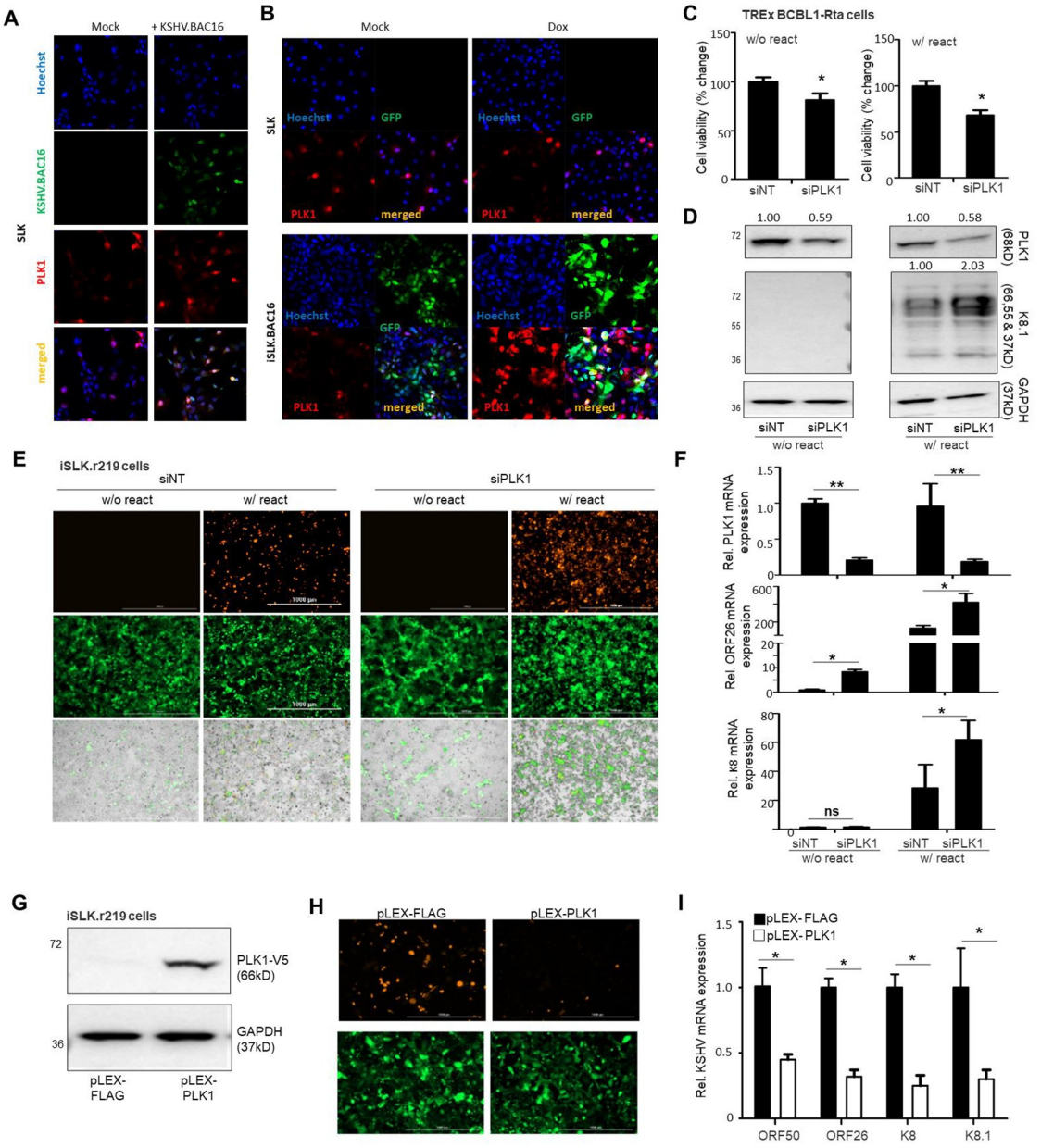

Fig 1. PLK1 plays a role in maintenance of KSHV latency. (A) SLK cells were *de novo* infected with KSHV.BAC16 viruses that were harvested from supernatant of iSLK.BAC16 cell treated with doxycycline (Dox). KSHV-infected SLK cells were fixed, stained with an anti-PLK1 primary antibody and an Alexa Fluor 647 labeled secondary antibody, followed by confocal fluorescence imaging. Nuclei were stained with Hoechst (blue), and GFP indicated cells that were infected with KSHV.BAC16 viruses (green). (B) SLK and iSLK.BAC16 cells were treated with Dox or mock, followed by the immunostaining of PLK1 and confocal fluorescence imaging. Images were one representative from three independent experiments. (C) TREx BCBL1-Rta cells were transiently transfected with the indicated siRNAs (siNT or siPLK1) and treated with Dox or mock to induce KSHV reactivation, followed by cell viability analysis. (D) Protein level of PLK1 and KSHV lytic gene K8.1 in above cells (C) was measured by immunoblotting. GAPDH was used as a loading control. (E) iSLK.r219 cells were transiently transfected with indicated siRNAs and treated with Dox or mock to induce KSHV reactivation. GFP (constitutively expressed from EF-1alpha promoter within KSHV genome) and RFP (expressed from KSHV PAN lytic promoter) signals in cells were visualized by fluorescence microscopy. (F) mRNA level of PLK1 and KSHV lytic genes (ORF26, K8) in above cells (E) were measured by RT-qPCR and normalized to GAPDH. (G) iSLK.r219 cells were transiently transfected with pLEX-FLAG or pLEX-PLK1 vector, and treated with Dox to induce KSHV reactivation. Expression of V5-PLK1 protein was confirmed by immunoblotting. (H) GFP and RFP signals in above cells (G) were visualized by fluorescence microscopy. (I) mRNA level of KSHV lytic genes (ORF50, ORF26, K8, K8.1) in above cells (G) were measured by RT-qPCR and normalized to GAPDH. Results were calculated from n = 3 independent experiments and presented as mean ± SD (* $p<0.05$, ** $p<0.01$; two-tailed paired Student t-test).

https://doi.org/10.1371/journal.ppat.1009764.g001

transiently transfected in iSLK.r219 cells, and its expression was confirmed by protein immunoblotting (Fig 1G) or RT-qPCR (S1F Fig). Overexpression of PLK1 led to significant reduction of Dox-induced KSHV lytic reactivation through measurement of RFP by fluorescent imaging (Fig 1H) or KSHV lytic genes expression (ORF50, ORF26, K8, K8.1) by RT-qPCR (Fig 1I).

Inhibition of PLK1 facilitates the KSHV lytic switch from latency

Our recent study demonstrated that chemical inhibition of PLK1 enable reactivation of latent HIV [15]. Since PLK1 depletion by siRNA facilitated KSHV lytic reactivation, we further confirm whether chemical inhibition of PLK1 yields similar effect. We used SBE 13 HCl (SBE), a PLK1-specific inhibitor, which targets inactive PLK1 conformation [18]. Consistent with the results of PLK1 depletion, SBE treatment led to further increase of Dox-induced KSHV lytic reactivation in TREx BCBL1-Rta cells in a dose dependent manner through measurement of KSHV K8.1 lytic protein by immunoblotting (Fig 2A) or lytic gene expression (ORF50, K8, K8.1) by RT-qPCR (Fig 2B). We also tested SBE in BCBL1 cells. BCBL1 cells were treated either with TPA/NaB or mock in the presence or absence of SBE. Treatment with SBE alone showed weak effect of KSHV lytic reactivation, but combination of TPA/NaB with SBE dramatically increase K8.1 protein expression, more than TPA/NaB alone (Fig 2C). Likewise, SBE treatment alone failed to reactivate latent KSHV but synergized with Dox to efficiently induce KSHV lytic reactivation in iSLK.r219 cells through measurement of RFP by fluorescent imaging (Fig 2D) or KSHV ORF45 lytic protein by immunoblotting (Fig 2E), although SBE treatment did not have any obvious cytotoxicity in these cells (S2A Fig). We further verified SBE's effect on promiting KSHV lytic reactivation through measurement of KSHV viral DNA copy number in supernatants from TPA/NaB-treated or un-treated BCBL1 (KSHV+) as well as BC-2 and HBL-6 (KSHV+, EBV+) cells (S2B Fig). Menahwile, SBE treatment had no obvious effect on PLK1 protein expression (S2C Fig).

Recently, PLK1-BET dual inhibitors have been developed to target both PLK1 and BRD4, two major protein targets for anticancer therapies [19,20]. We tested one of such PLK1-BET dual inhibitors, UMB-158, which possesses the novel scaffold (UMB series) [21] and was recently shown to reactivate latent HIV by our group [15]. As expected, UMB-158 treatment also amplified the effect of Dox-induced KSHV lytic reactivation in TREx BCBL1-Rta cells in a dose dependent manner (Fig 2F). We then tested two other PLK1-BET dual inhibitors, BI-6727 and BI-2536 that also reactivate latent HIV [22]. Both of these PLK1-BET dual inhibitors enhanced Dox-induced KSHV lytic reactivation (S2D Fig) in agreement with all other PLK1 inhibitors.

Inhibition of PLK1 promotes the cell death of KSHV-reactivated tumor cells

Several reports provide evidences that PLK1 supports cell survival [23,15]. Thus, we wondered whether inhibition of PLK1 may generate a synergistic "killing" effect with viral cytopathic effect caused by KSHV reactivation to promote cell death of lytic-reactivated tumor cells. Indeed, we identified that SBE treatment caused increase of cell death of TREx BCBL1-Rta cells undergoing Dox-induced KSHV lytic reactivation in comparison to mock treatment measured by the LIVE/DEAD assay (Fig 3A). In parallel, we observed that SBE treatment led to a greater reduction of cell viability in Dox-treated TREx BCBL1-Rta cells in comparison with mock treatment measured by ATP assay eventhough the cell viability of both cases were lower than BJAB cells, a KSHV/EBV-negative B lymphoma cell line, which underwent the same treatments (S3A Fig). The same effect of SBE was observed in TPA/NaB-treated vs un-treated

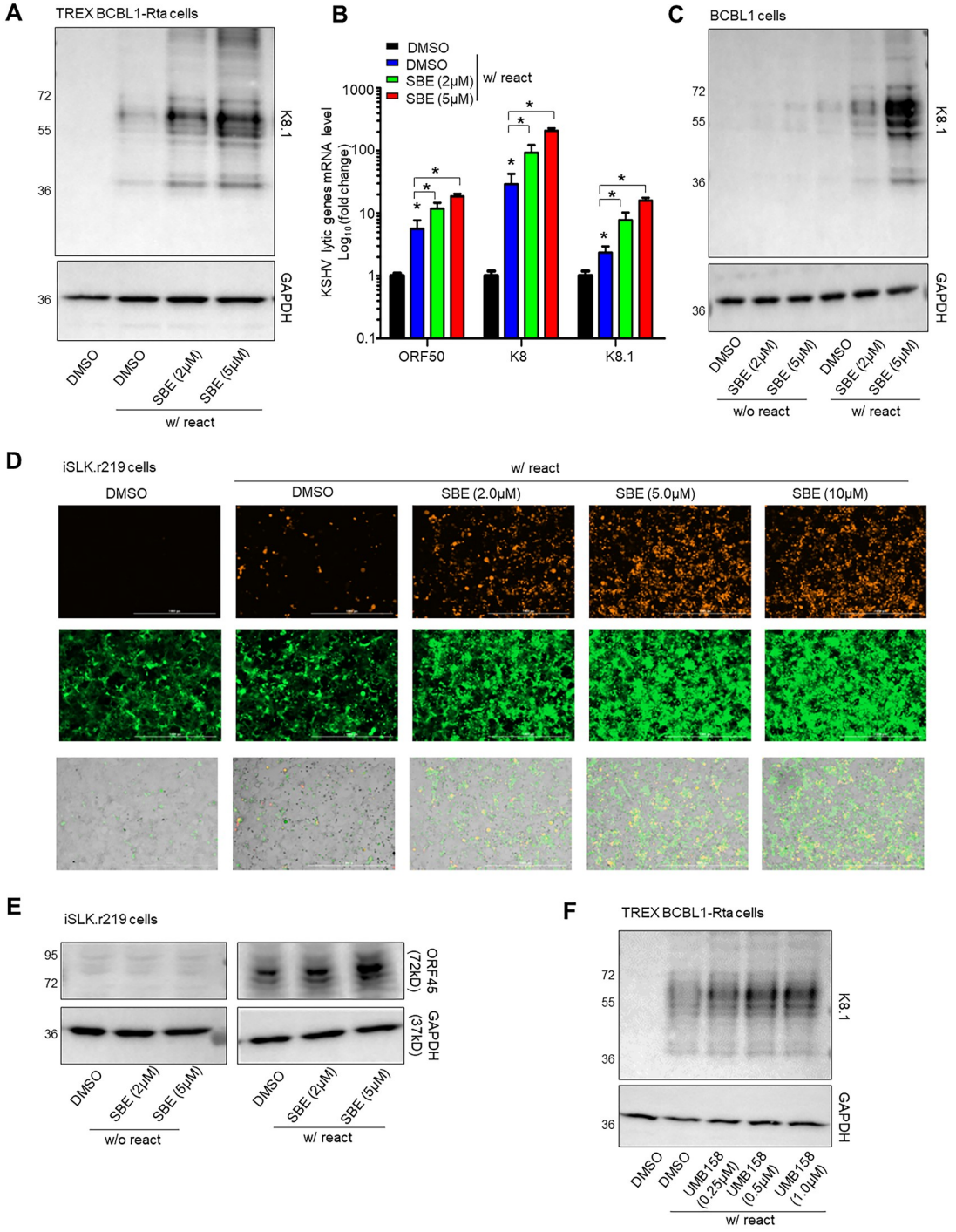

Fig 2. PLK1 inhibition facilitates lytic switch of latent KSHV. (A) TREx BCBL1-Rta cells were treated with the PLK1-specific inhibitor, SBE 13 HCl (SBE), and Dox to induce KSHV reactivation. Protein level of KSHV K8.1 was measured by immunoblotting. GAPDH was used as a loading control. (B) mRNA level of KSHV lytic genes (ORF50, K8, K8.1) in above cells (A) were measured by RT-qPCR and normalized to GAPDH. Results were calculated from n = 3 independent experiments and presented as mean ± SD (* $p<0.05$, treatment vs DMSO only and as specified; two-way ANOVA). (C) BCBL1 cells were treated with SBE or DMSO, in the presence or absence of TPA (20ng/ml) + sodium butyrate (TPA/NaB) (1mM) to induce KSHV reactivation. Protein level of KSHV K8.1 was measured by immunoblotting. GAPDH was used as loading control. (D) iSLK.r219 cells were treated with SBE or DMSO, and Dox to induced KSHV reactivation. GFP and RFP signals in these cells were visualized by fluorescence microscopy. (E) Protein level of KSHV lytic gene ORF45 in iSLK.r219 cells +/- SBE and +/- Dox was measured by immunoblotting. GAPDH was used as a loading control. (F) TREx BCBL1-Rta cells were treated with the PLK1/BET dual inhibitor, UMB-158, and Dox to induce KSHV reactivation. Protein level of KSHV K8.1 was measured by immunoblotting. GAPDH was used as a loading control.

https://doi.org/10.1371/journal.ppat.1009764.g002

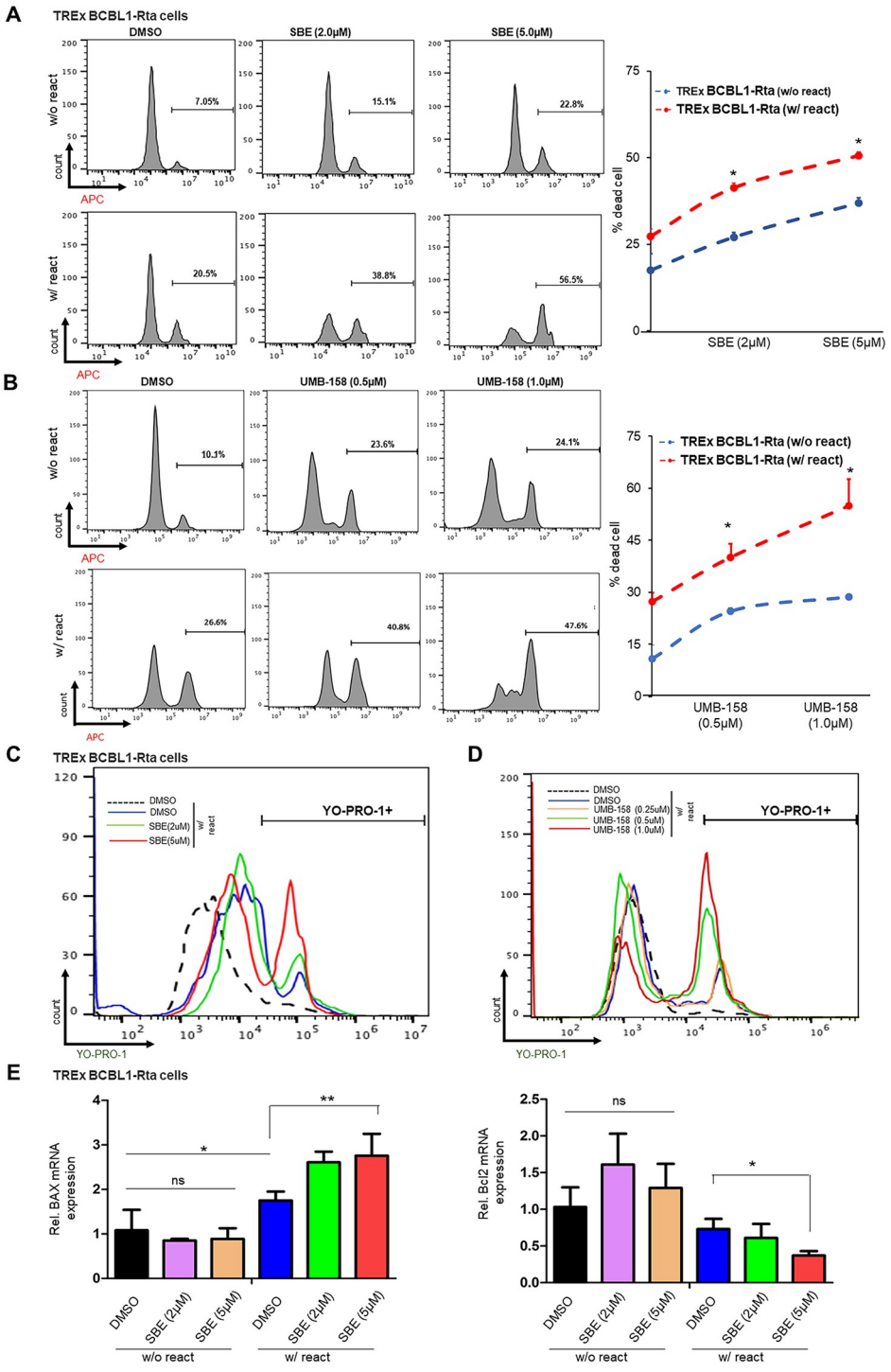

Fig 3. PLK1 inhibition promotes death of KSHV-reactivated cells. (A, B) TREx BCBL1-Rta cells were treated with SBE (A), UMB-158 (B), or DMSO, in the presence or absence of Dox to induce KSHV reactivation. Percentage of dead cells was measured by LIVE/DEAD staining, followed by flow cytometry analysis. (C, D) TREx BCBL1-Rta cells were treated with SBE (C), UMB-158 (D), or DMSO, and induced with Dox. Percentage of apoptotic cells was measured by YO-PRO-1 staining, followed by flow cytometry analysis. (E) mRNA level of apoptosis-related genes, BAX and Bcl2, in TREx BCBL1-Rta cells +/- SBE and +/- Dox were measured by RT-qPCR and normalized to GAPDH. Results were calculated from n = 3 independent experiments and presented as mean ± SD (ns: not significant, * $p<0.05$, ** $p<0.01$; two-tailed paired Student t-test).

https://doi.org/10.1371/journal.ppat.1009764.g003

BCBL1 cells with the cell viability of BCBL1 cells without TPA/NaB induction is similar to that of BJAB cells (S3B Fig). We decided to test dual inhibition of PLK1/BET as well. UMB-158 promoted more cell death comparable to the effect of SBE in TREx BCBL1-Rta cells pre-treated with Dox to reactivate latent KSHV when compared to mock treatment (Fig 3B). Coincide with more cell death, UMB-158 treatment showed greater reduction of cell viability in Dox-treated TREx BCBL1-Rta cells in comparison to mock treatment as measured by the ATP assay (S3C Fig). We further confirmed that treatment of Dox-treated TREx BCBL1-Rta cells with other PLK1-BET dual inhibitors, BI-6727 and BI-2536, reduced cell viability, especially at the higher dose (S3D Fig).

To determine whether SBE and UMB-158 promotes cell death of KSHV-reactivated tumor cells via cell apoptosis, we used YO-PRO-1 and propidium iodide (PI) dual staining assays. Apoptotic cells become permeant to green-fluorescent YO-PRO-1, while permissibility of red-fluorescent PI indicates necrotic cell death. Indeed, treatment of SBE (Figs 3C and S3E) or UMB-158 (Figs 3D and S3F) led to more cell death and apoptosis of KSHV-reactivated TREx BCBL1-Rta cells when compared to DMSO by measuring fluorescence intensity at PE and FITC channels respectively. Furthermore, we also measured the effect of SBE on gene expression of the pro-apoptotic gene BAX [24] and the anti-apoptotic gene BCL2 [25]. SBE, especially at the higher dose (5μM), led to upregulation of BAX gene and downregulation of Bcl2 gene in reactivated TREx BCBL1-Rta cells but not in mock-treated cells (Fig 3E).

Inhibition of PLK1 destabilizes c- Myc and affects histone methylation

The proto-oncogene myc encodes c-Myc, a transcription factor, which regulates cellular growth, proliferation, differentiation, and apoptosis [26,14]. It is known that PLK1 regulates c-Myc activities [27,14], while c-Myc suppresses KSHV lytic reactivation [28]. To evaluate the role of c-Myc in mediating the effect of PLK1 inhibition on promoting KSHV lytic reactivation and cell death of KSHV-reactivated cells, we measured protein level of c-Myc in iSLK.BAC16 and iSLK.r219 cells treated with SBE, which led to reduction of c-Myc protein in these cells in a dose-dependent manner (Fig 4A and 4B). We then tried to measure c-Myc protein in TREx BCBL1-Rta cells with similar approach. However, the exogenous Rta protein is Myc-tagged in these cells, which interferes with detection of endogenous c-Myc. In parallel, we showed that SBE treatment downregulated expression of certain Myc-dependent cell-cycle genes, including cyclin A and E (S4A Fig), in Dox-treated, KSHV-reactivated TREx BCBL1-Rta cells that further reduced their cell survival.

It is known that c-Myc modulates activities of histone lysine methyltransferases [29]. Meanwhile, it has been reported that two inactive histone marks, H3K27me3 and H3K9me3, are involved in maintenance of KSHV latency [30]. Therefore, we speculated that inhibition of PLK1 further modulates the above histone marks via destabilization of c-Myc. Our data showed that SBE treatment resulted in the reduction of overall H3K27me3 but not H3K9me3 histone mark in both iSLK.BAC16 and iSLK.r219 cells (Fig 4A and 4B). In SBE-treated TREx BCBL1-Rta cells, overall H3K27me3 was also significantly reduced at the higher dose of SBE (5 μM), while it only caused a mild reduction of H3K9me3 (Fig 4C). Furthermore, we determined the effect of SBE on local level of the above histone marks (H3K27me3, H3K9me3) and PLK1 at promoter region of KSHV lytic genes (ORF50, ORF59) as well as the lytic origin of KSHV DNA replication (OriLyt) by ChIP-PCR. Our results showed that SBE treatment significantly reduced the level of H3K27me3 (Fig 4D) and PLK1 (Fig 4E) at all tested loci of KSHV episomes, but not H3K9me3 (S4B Fig).

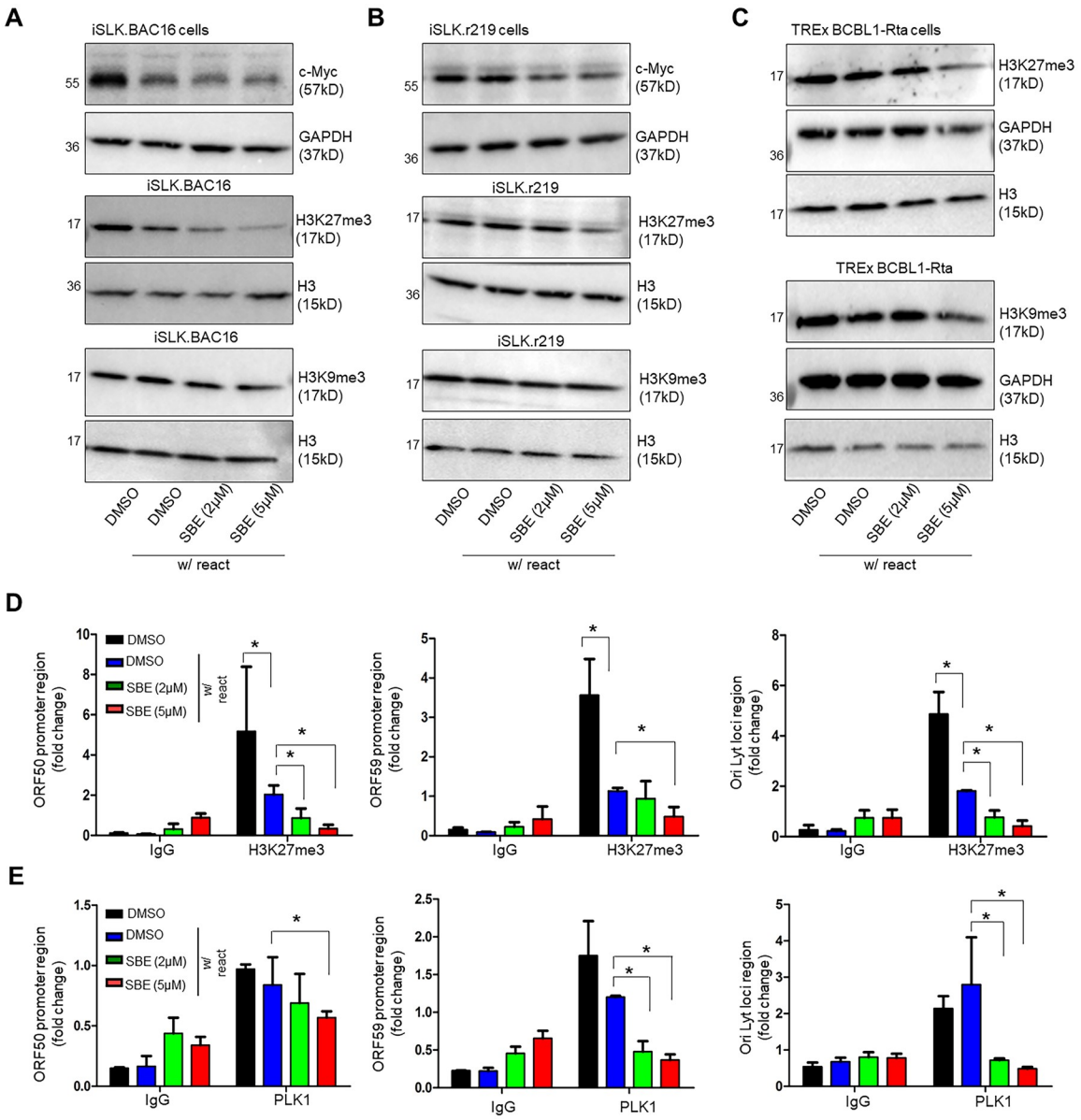

Fig 4. PLK1 inhibition destabilizes c-Myc and reduces H3K27me3. (A-C) Protein level of c-Myc, H3K27me3, H3K9me3, or H3 in iSLK.BAC16 (A), iSLK.r219 (B), or TREx BCBL1-Rta (C) cells was measured by immunoblotting. These cells were treated with SBE or DMSO, and Dox to induce KSHV reactivation. GAPDH was used as the loading control. (D, E) TREx BCBL1-Rta cells were treated with SBE or DMSO, and Dox to induce KSHV reactivation. Cell lysates were prepared and subjected to ChIP assay by using antibodies against H3K27me3, PLK1, or a mouse IgG as a negative control. Precipitated DNA samples were further analyzed by qPCR by using primers targeting promoter region of KSHV lytic genes (ORF50, ORF59) and OriLyt, and normalized to IgG control. Results were calculated from n = 3 independent experiments and presented as mean ± SD (* $p<0.05$; two-tailed paired Student t-test).

https://doi.org/10.1371/journal.ppat.1009764.g004

Inhibition of PLK1 and STAT3 leads to efficient KSHV lytic switch from latency

As we described previously, inhibition of PLK1 alone was not sufficient to induce efficient KSHV lytic reactivation but rather augmented it when combined with other latency-reversing agents (LRAs). It has been reported that STAT3 inhibition is sufficient to induce KSHV lytic

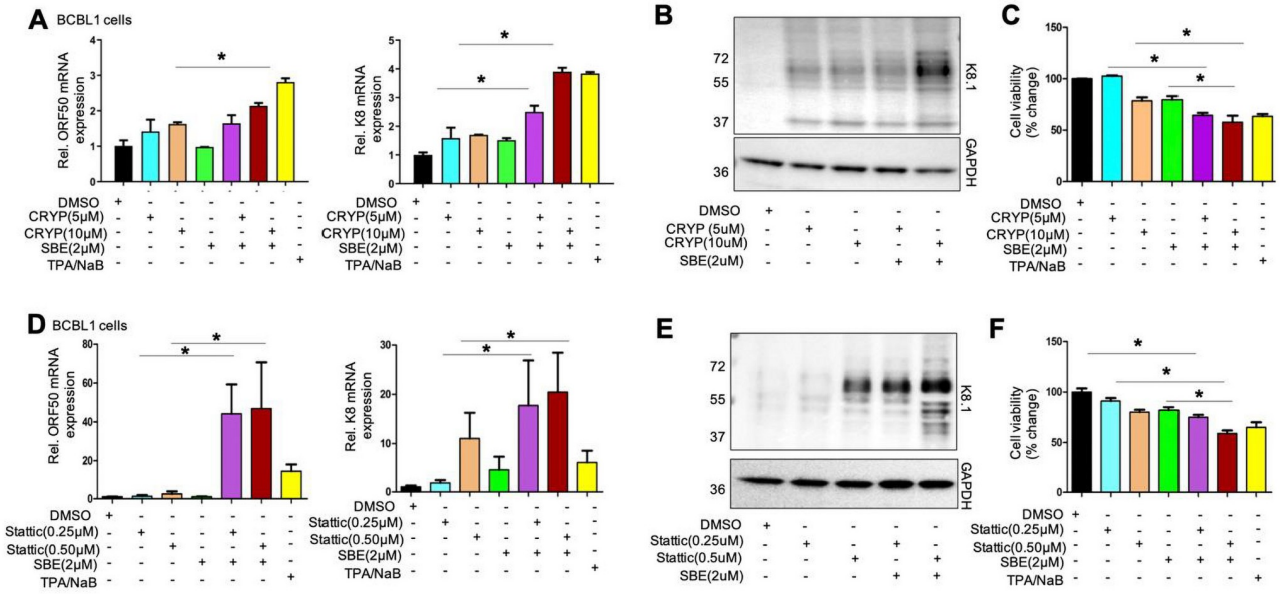

Fig 5. Inhibition of PLK1 and STAT3 efficiently induces KSHV lytic reactivation. (A, D) BCBL1 cells were treated with cryptotanshinone (CRYP, A) or stattic (D) in the presence or absence of SBE. TPA/NaB treatment was used as a positive control to reactivate latent KSHV. mRNA level of KSHV lytic genes (ORF50, K8) in these cells were measured by RT-qPCR and normalized to GAPDH. (B, E) Protein level of KSHV K8.1 in above cells (A, D) was measured by immunoblotting. GAPDH was used as loading control. (C, F) Cell viability of above cells (A, D) was measured by ATP-based assays and normalized to DMSO. Results were calculated from n = 3 independent experiments and presented as mean ± SD (* $p<0.05$; two-tailed paired Student t-test).

https://doi.org/10.1371/journal.ppat.1009764.g005

reactivation [31]. STAT3 inhibitors have shown the promising anticancer potency and are currently under evaluation in clinical trials [32]. We further tested whether the combinatory inhibition of PLK1 and STAT3 has more potent effect to reactivate KSHV lytic phase. Our studies involved two STAT3 inhibitors, cryptotanshinone (CRYP) and stattic, which have been demonstrated to reactivate latent KSHV [33,34]. BCBL1 cells were treated with CRYP (5, 10μM) or stattic (0.25, 0.5μM) alone or in combination with SBE at the lower dose (2μM). CRYP treatment alone had a moderate KSHV latency-reversing potency, but its combination with SBE showed greater effect in BCBL1 cells through measurement of KSHV lytic gene expression (ORF50, K8) by RT-qPCR (Fig 5A) as well as K8.1 lytic protein level by immunoblotting (Fig 5B). Along with more lytic reactivation, we also saw reduction of cell viability in the combination treatments as measured by the ATP assay (Fig 5C). More striking effects were observed when combination of stattic with SBE was used. This combination created a strong KSHV latency-reversing effect superior to the positive control (TPA/NaB treatment) in BCBL1 cells (Fig 5D and 5E), which also correlated with significant reduction of cell viability (Fig 5F). In addition, combination of CRYP or static with SBE amplified the effect of TPA/NaB-induced KSHV lytic reactivation in BCBL1 cells (S5 Fig).

Inhibition of PLK1 promotes EBV lytic switch and cell death of EBV + tumor cells

As KSHV shares certain similarities to EBV in host regulation of viral latency and lytic replication [35], we aimed to determine whether PLK1 also regulates EBV lytic switch from latency. We depleted endogenous PLK1 protein in Akata-BX1 cells by transient transfection of its shRNA (shPLK1) or non-target shRNA (shNT) using TurboFect transfection reagent, whose

knockdown efficiency was confirmed by immunoblotting (Fig 6A). Such PLK1 knockdown led to higher expression EBV ZEBRA protein (Fig 6A) as well as expression of a series of EBV lytic genes measured by RT-qPCR (Fig 6B) in Akata-BX1 cells treated with human IgG (hIgG) to reactivate latent EBV. Moreover, treatment of SBE (Fig 6C) or UMB-158 (Fig 6D) further promoted cell death and reduced cell viability (S6A and S6B Fig) of hIgG-treated, EBV-reactivated Akata-BX1 cells, which correlated with enhanced EBV lytic reactivation through measurement of EBV ZEBRA protein (Fig 6E and 6F). We verified SBE's effect on promiting EBV lytic reactivation through measurement of EBV viral DNA copy number in supernatants from TPA/NaB-treated or un-treated BC-2 and HBL-6 (KSHV+, EBV+) cells (S6C Fig). We also observed that combination of STAT3 inhibitors (CRYP, stattic) with SBE led to more reduction in cell viability (Fig 6G) as well as increased level of EBV ZEBRA protein in Akata-BX1 cells (Fig 6H). Finally, combination of CRYP or stattic with SBE further augmented the effect of hIgG-induced EBV lytic reactivation in Akata-BX1 cells (S6D Fig).

PLK1 expression in B cells is elevated in the context of HIV infection

KSHV infection is more common among people living with HIV (PLWH) than in general population [36]. Since the incidence of B-cell lymphoma among HIV-infected subjects greatly exceeds that of the general population [37], we decided to compare PLK1 expression in B cell lymphoma samples from both HIV-negative and positive subjects. PLK1 mRNA abundance were found to be markedly elevated in HIV-positive lymphoma samples compared to HIV-negative samples (Fig 7A). This observation guided us to specifically investigate the role of PLK1 expression in B cells between HIV-negative and positive subjects. B cells were isolated from peripheral blood mononuclear cells (PBMCs) of these donors (Fig 7B), and PLK1 mRNA and protein levels were measured by qPCR and immunostaining respectively. Increased of PLK1 mRNA level (Fig 7C) was consistent across HIV+ subjects compared to the healthy donors. Increased of PLK1 protein level was also observed in HIV+ subjects (Fig 7D and 7E). We further determined the impact of HIV infection on PLK1 expression in B cells *in vitro*. Jurkat cells were subjected to HIV-1 IIIB infection, verified by immunoblotting of HIV-1 Gag p24 protein (S7A Fig). HIV-infected Jurkat cells were co-cultured with CFSE-stained BJAB cells, which led to a moderate increase of PLK1 protein level measured by IFAs when compared to BJAB cells co-cultured with non-infected Jurkat cells (Fig 7F).

We previously showed that HIV Nef protein contributes to the upregulation of PLK1 in HIV-infected T cells [15]. Nef is a ~27 kDa myristoylated protein encoded by the highly variable *nef* gene located at the 3' end of HIV genome. Following HIV infection or upon HIV viral reactivation, Nef is expressed as one of the earliest and most abundant viral proteins [38]. Nef can be secreted from infected or transfected cells, and detected in the plasma of HIV-infected individual even with unobservable level of plasma HIV RNA because of the cART suppression [39,40]. The general consensus is that peripheral Nef protein is produced by HIV-infected cells located in lymphoid tissues as a major HIV reservoir [41]. Recent report has shown that HIV Nef protein promotes latent infection of KSHV [42], which was confirmed by our results that treatment of recombinant Nef (rNef) protein suppressed KSHV lytic reactivation in Dox-treated TREx BCBL1-Rta cells without any cytotoxicity (S7B and S7C Fig). Such function of Nef is in line with PLK1's role in regulating KSHV latency. Thus, we expected that Nef is the HIV viral protein that mediates the PLK1 induction in B cells. BJAB cells were treated with rNef protein at the increasing dose, which indeed resulted in the upregulation of PLK1 protein (**Fig 7G**). Lastly, similar effects were observed in Akata-BX1 (**Fig 7H**) and TREx BCBL1-Rta (**Fig 7I**) cells treated with rNef protein.

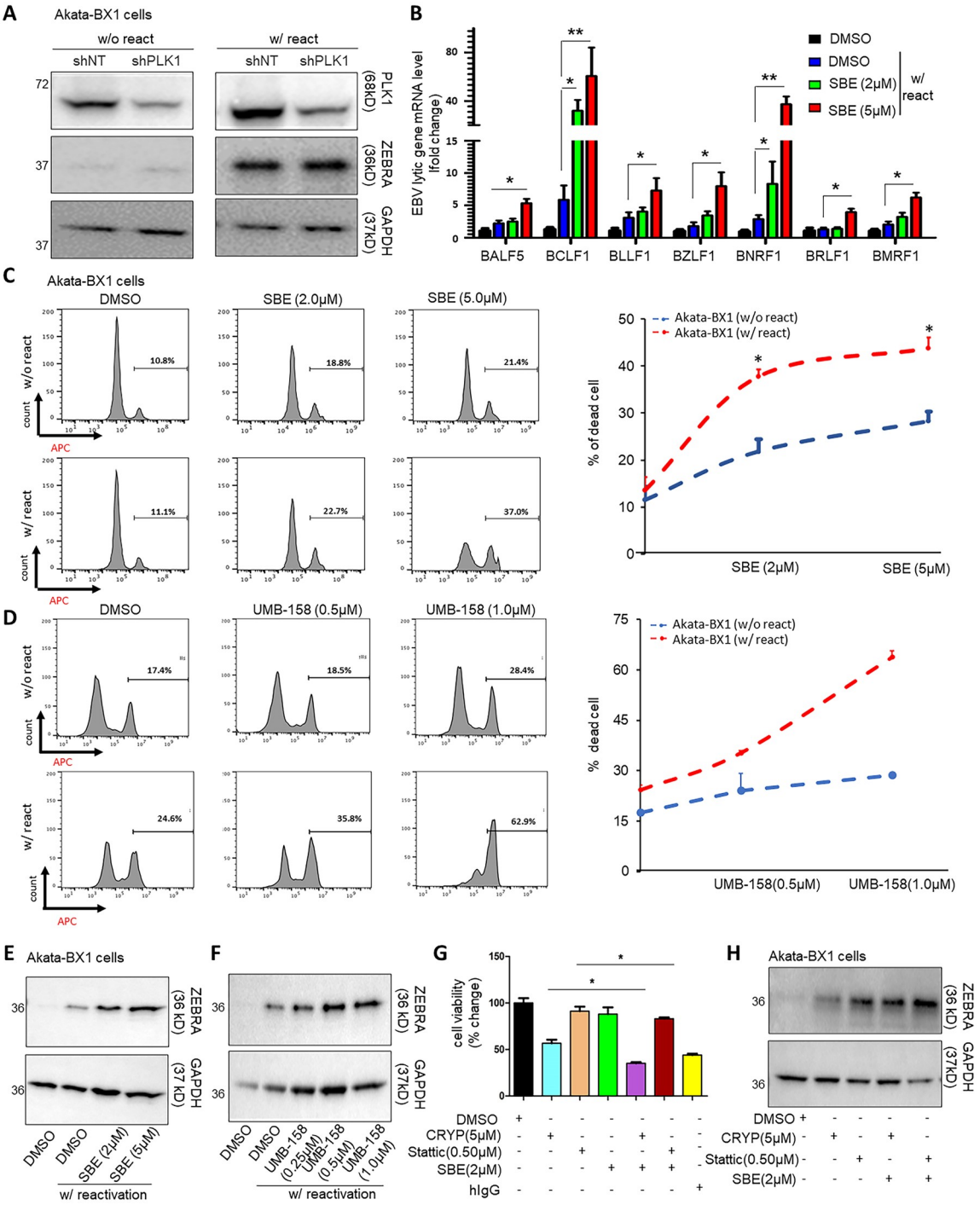

Fig 6. Inhibition of PLK1 benefits EBV reactivation and promotes death of EBV-reactivated tumor cells. (A) Akata-BX1 cells were transiently transfected with the pINDUCER10 vector expressing indicated shRNAs (shNT or shPLK1) using TurboFect transfection reagent, and treated with Dox to induce shRNA expression as well as human IgG (hIgG) to induce EBV reactivation. Protein level of PLK1 and EBV lytic gene ZEBRA was measured by immunoblotting. GAPDH was used as a loading control. (B) mRNA level of indicated EBV lytic genes was measured by RT-qPCR and normalized to GAPDH. Results were calculated from n = 3 independent experiments and presented as mean ± SD (* $p<0.05$, ** $p<0.01$; two-way ANOVA). (C, D) Akata-BX1 cells were treated with SBE (C), UMB-158 (D), or DMSO, in the presence or absence of hIgG. Percentage of dead cells was measured by LIVE/DEAD staining, followed by flow cytometry analysis. (E, F) Protein level of EBV ZEBRA in above cells (C, D) was measured by immunoblotting. GAPDH was used as a loading control. (G) Akata-BX1 cells were treated with CRYP or stattic in the presence or absence of SBE. hIgG treatment was used as a positive control to reactivate latent EBV. Cell viability of these cells was measured by ATP-based assays and normalized to DMSO. (H) Protein level of EBV ZEBRA in above cells (G) was measured by immunoblotting. GAPDH was used as a loading control.

https://doi.org/10.1371/journal.ppat.1009764.g006

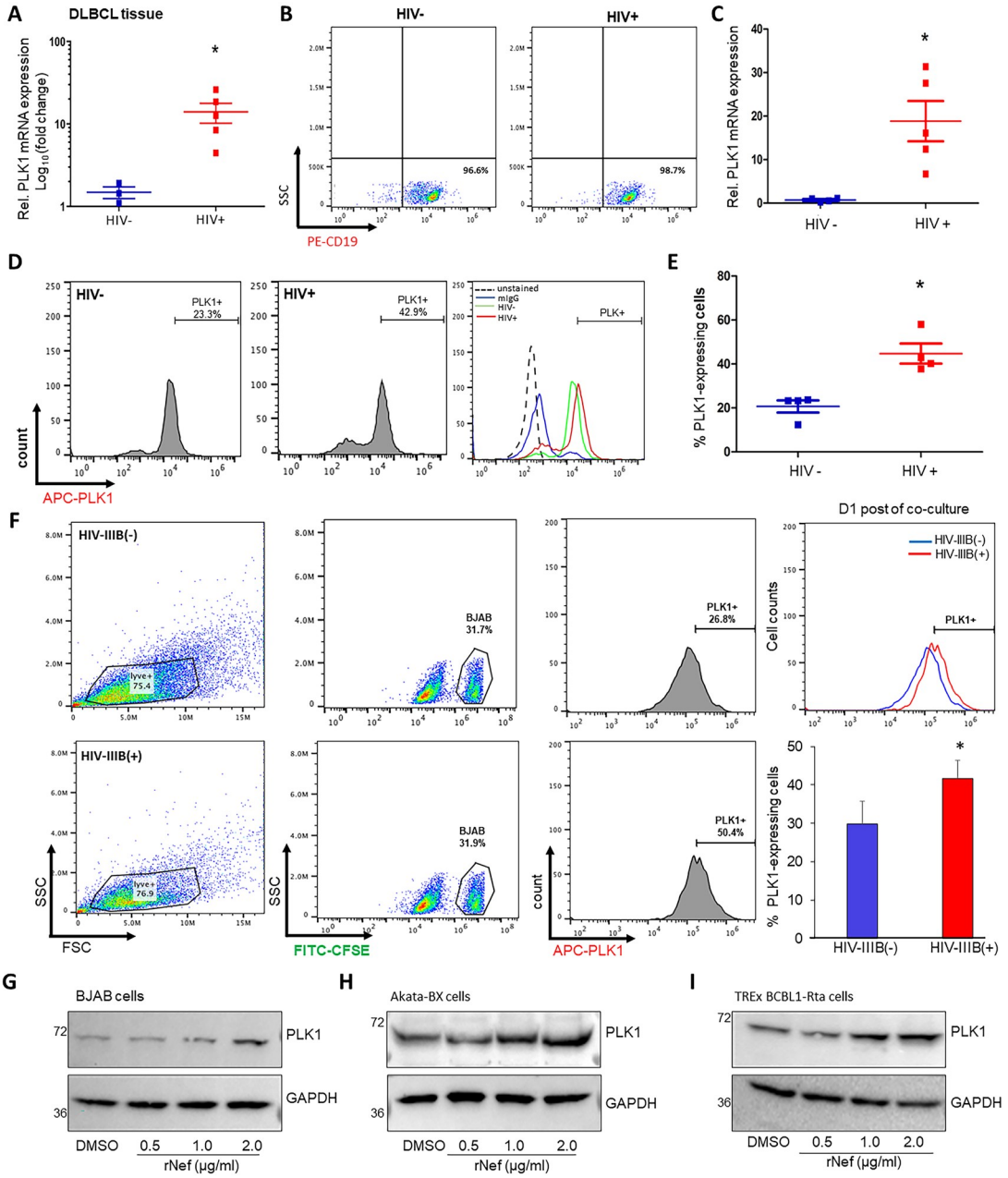

Fig 7. PLK1 expression is induced in B cells in the context of HIV infection. (A) Total RNAs were extracted from the fixed diffuse large B-cell lymphoma (DLBCL) tissue samples of HIV-negative (HIV-, n = 3) and HIV-positive (HIV+, n = 5) individuals. mRNA level of PLK1 in these tissue samples was measured by RT-qPCR and normalized to GAPDH. (B) A PE-conjugated CD19 antibody was used for B cell enrichment from PBMCs of HIV-infected, aviremic patients (HIV+, n = 5) or healthy donors (HIV-, n = 5). Purity of isolated $CD19^{+}$ B cells was confirmed by flow cytometry analysis. (C) mRNA level of PLK1 in above isolated B cells (B) was measured by RT-qPCR and normalized to GAPDH. (D) Protein level of intracellular PLK1 in above isolated B cells (B) was measured by immunofluorescence. Percentage of PLK1-expressing cells was determined by flow cytometry analysis. (F) HIV-1 IIIB infected Jurkat cells were co-cultured with BJAB cells that were pre-stained with CFSE. Protein level of intracellular PLK1 in CFSE-labeled BJAB cells was measured by immunofluorescence. Percentage of PLK1-expressing cells was determined by flow cytometry analysis. (G-I) Protein level of PLK1 in BJAB (G), Akata-BX1 (H), or TREx BCBL1-Rta (I) cells treated with recombinant Nef (rNef) protein at the increasing dose or DMSO was measured by immunoblotting. GAPDH was used as loading control. Results were calculated from n = 3 independent experiments and presented as mean ± SD (* $p<0.05$; two-tailed paired Student t-test).

https://doi.org/10.1371/journal.ppat.1009764.g007

Inhibition of PLK1 reduces viral reservoirs of KSHV and EBV in B cells

Our results have shown that PLK1 inhibition augments lytic switch of KSHV/EBV latency and promotes cell death of KSHV/EBV-infected B lymphoma cells undergoing viral reactivation, thus we expected that use of PLK1 inhibitors facilitates the reduction or elimination of KSHV/EBV viral reservoirs in these cells. To test this, we prepared a serial dilution of BCBL1 (KSHV +) or Akata-BX1 (EBV+) cells within the KSHV/EBV-negative BJAB cells. BCBL1:BJAB (Fig 8A) and Akata-BX1:BJAB (Fig 8B) cell mixtures were treated with TPA/NaB and hIgG respectively to induce viral reactivation in the presence or absence of SBE. It was evident that addition of SBE to KSHV/EBV LRAs led to significant reduction of KSHV/EBV viral reservoirs in B cells through measurement of viral DNA copy number by RT-qPCR. Surprisingly, treatment of SBE alone also showed similar reduction in these cell mixtures (S8 Fig), which suggests that PLK1 inhibition can actually induce, albeit weakly, certain level of viral reactivation of KSHV and EBV in these cells.

Discussion

In this study, we have shown that both KSHV *de novo* infection and lytic switch from latency lead to induction of PLK1 (Figs 1A and 1B and S1A and S1B). Our earlier investigation have found that HIV infection induces PLK1 in a PI3K-depdenent manner [15]. Interestingly, several KSHV proteins, including K1, viral G protein-coupled receptor (vGPCR), vIL-6, and ORF45, have been shown to activate PI3K as well [43]. In addition, these KSHV viral proteins also participate in latent and lytic switch, which would likely result in PLK1 induction. Here, we show that HIV Nef protein is able to induce PLK1 upregulation in B cells (Fig 7G-I). Exposure of PEL cells to soluble Nef protein was shown to inhibit lytic replication and promote latency of KSHV, which is similar to PLK1's phenotypes. It has been also reported that Nef binds to the regulatory subunit (p85) of PI3K and activates Nef-associated p21-activated kinase (PAK) [44]. Given all these data, we speculate that induction of PLK1 represent the interaction mechanism between HIV and KSHV.

Further, it has been reported that co-infection of KSHV and HIV strongly correlates with cancer progression [45]. Based on our results, it is highly plausible that autocrine mechanism from KSHV infection and paracrine stimulation from HIV Nef protein coordinate to induce PLK1 to benefit KSHV persistent infection and survival of KSHV-infected B lymphocytes. Although it was not tested in the current study, EBV infection likely causes PLK1 induction as well since it has been shown that certain EBV lytic and latent proteins are capable of PI3K activation [46].

A key finding of our studies is that PLK1 promotes viral latency of gamma-herpesviruses since its depletion (Figs 1C-F and 6A and 6B and S1D and S1E Fig) or inhibition (Figs 2 and 6E and 6F, S2B and S2D and S6C Figs) facilitates viral lytic switch from latency for both KSHV and EBV. Our further mechanistic investigation unraveled that such inhibitory function of PLK1 is likely through regulation of c-Myc protein and histone methylations, particularly H3K27me3 (Fig 4). It is known that c-Myc is deregulated in ~30% of human cancers, including B and T cell lymphomas [26,47], and that it is required for maintenance of viral latency of both KSHV [28] and EBV [48]. More importantly, there are several reports delineating the role of PLK1 in regulation of c-Myc. PLK1 inhibition can result in the destabilization of c-Myc protein [27] as well as reduction of c-Myc phosphorylation, which interferes with its transcriptional activities [49]. It is still not clear how exactly c-Myc contributes to viral latency of KSHV and EBV. However, there are several studies suggesting that c-Myc modulates histone lysine methyltransferases (EZH2, G9a) that count for histone H3 methylations, H3K9me3 and H3K27me3 [50]. Interestingly, our results showed that PLK1 inhibition results in the

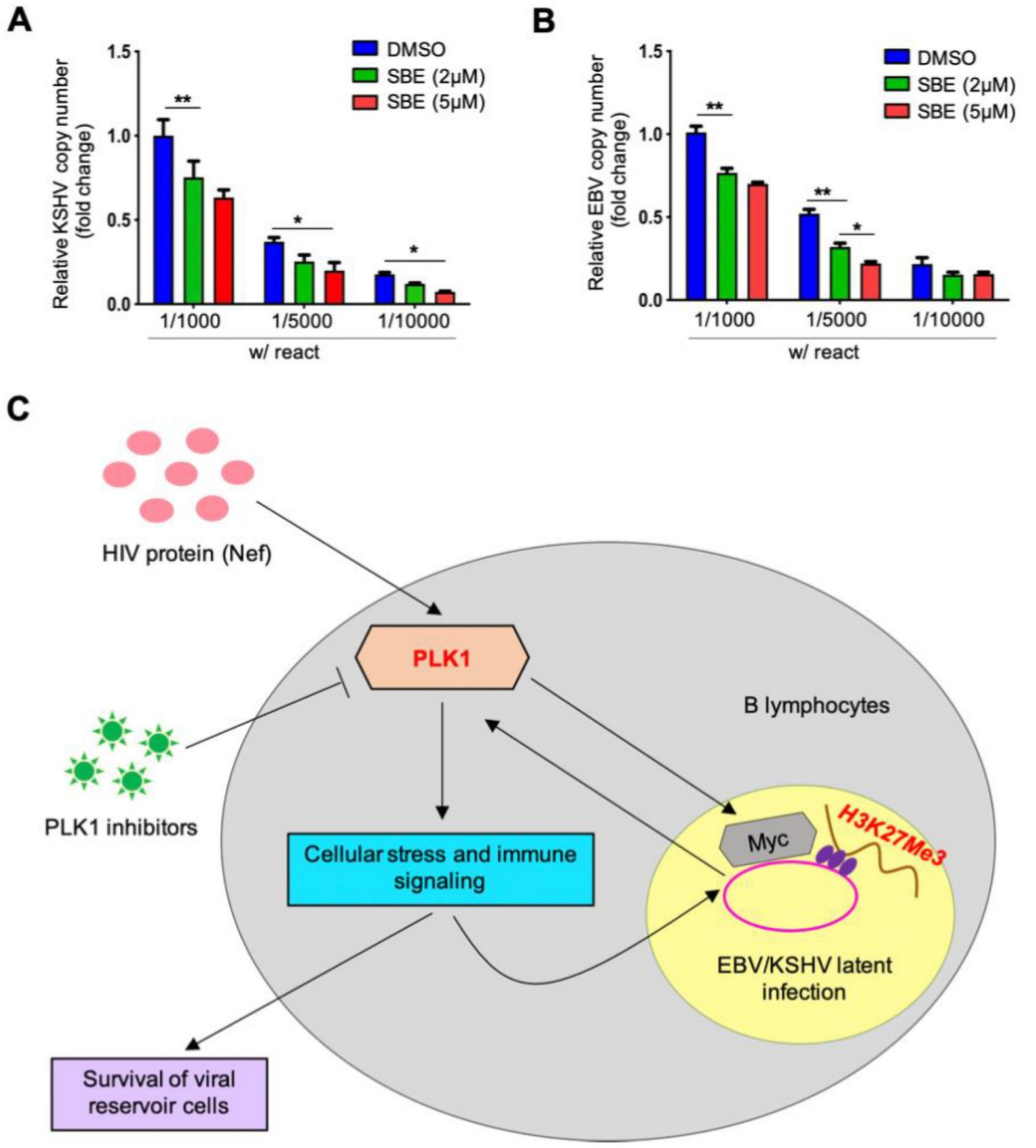

Fig 8. Inhibition of PLK1 reduces KSHV/EBV viral reservoirs in B cells. (A, B) A serial dilution of TREx BCBL1-Rta (A) or Akata-BX1 (B) cells within KSHV/EBV-negative BJAB cells was prepared, followed by treatment of Dox or hIgG respectively to induce viral reactivation, in the presence or absence of SBE. Copy number of viral DNA genome was measured by qPCR using primers that target ORF73/LANA (KSHV) or EBNA1 (EBV) respectively, and normalized to GAPDH. Results were calculated from n = 3 independent experiments and presented as mean ± SD (* $p<0.05$, ** $p<0.01$; two-tailed paired Student t-test). (C) A schematic model illustrating the roles of PLK1 in regulating viral latency of human gamma-herpesviruses. PLK1 expression is induced by KSHV infection or in the scenario of HIV infection. PLK1 upregulation would not only support the maintenance of KSHV latency via stabilization of c-Myc and thus increase of H3K27me3 level, but also boost survival of KSHV-infected tumor cells via PLK1's known multifaceted roles in regulating cellular stress and immune signaling. Hence, PLK1 inhibitors would facilitate lytic switch of KSHV latency and promote death of KSHV-reactivated tumor cells, overall inducing an efficient viral oncolysis and resulting in "killing" of KSHV-infected tumor cells as well as reduction of KSHV viral reservoirs. PLK1 may play such similar roles in regulation of EBV viral latency as well.

https://doi.org/10.1371/journal.ppat.1009764.g008

significant reduction of H3K27me3 at both global and local levels at KSHV lytic loci (Fig 4), but not H3K9me3 (S4B Fig). Indeed, H3K27me3 inactive mark associates with repressed transcription of KSHV lytic genes [51]. Above all, our studies demonstrated a previously unreported role of PLK1-c-Myc-H3K27me3 regulatory axis in promoting KSHV latency. Although it was not tested in our studies, such signaling likely has a similar impact on EBV latency given that c-Myc was recently shown to contribute to EBV latency [48].

PLK1 also plays a critical role in supporting cell survival, hence we noticed that PLK1 inhibition further promotes the death of KSHV/EBV-reactivated B lymphoma cells (Figs 3A and 3B and 6C and 6D and S3 Fig). However, we also showed that PLK1 inhibition (S1C and S2A Figs) yields no obvious effect on cell death of parental SLK cells and SLK cells harboring latent KSHV although it still facilitated KSHV lytic reactivation in these cells (Fig 2). It is likely due to different sensitivity that different types of cells possess to the loss or inhibition of PLK1. Nevertheless, our results clearly demonstrated that PLK1 inhibition would really benefit the viral oncolysis approach to treat KSHV/EBV-positive B lymphomas, especially since KSHV infection would cause PLK1 induction in these cells. PLK1 can contribute to cell survival through multiple mechanisms. As shown by our results (Fig 3E), PLK1 inhibition deregulated expression of apoptosis-related genes (BAX, BCL2), indicating that cell apoptosis is one major type of cell death induced by PLK1 inhibition. We also showed that PLK1 inhibition causes destabilization of c-Myc that may contribute to the release of cell cycle brakes [52], thus interfering with cell cycle progression. In fact, our results demonstrated that PLK1 inhibition suppresses the expression of cyclin gene expression under c-Myc regulation (S4A Fig). PLK1's role in this aspect with relevance to KSHV/EBV pathogenesis will be further investigated in future studies.

As we previously noted, depletion or inhibition of PLK1 alone is not sufficient to induce KSHV/EBV lytic reactivation. The experimental reagents, such as Dox, hIgG, and TPA/NaB, are not appliable for actual use in clinic. Therefore, we seek for other compounds that are capable of viral reactivation for KSHV/EBV and also suitable for potential future clinical use. Recently, it has been reported that KSHV infection induces STAT3 phosphorylation [53] and inhibition of STAT3 causes KSHV reactivation in B lymphoma cells [31]. Some of STAT3 inhibitors are currently under evaluation in clinical trials for treating cancers [54,32]. Our results showed that combination of PLK1 and STAT3 inhibitors (CRYP, Stattic) is promising to efficiently induce not only lytic reactivation of both KSHV (Fig 5A, 5B, 5D and 5E) and EBV (Fig 6H) but also cell death of KSHV/EBV-reactivated B lymphoma cells (Figs 5C and 5F and 6G). This formulates an attractive regimen to specifically target KSHV/EBV-infected tumor cells. Latent KSHV/EBV are reactivated to trigger death of the infected cells constitutes the viral oncolytic approach, which itself is worthy of further investigation *in vivo*. In particular, the PLK1-induced oncolysis would benefit HIV-infected individuals even more since our earlier results also showed that PLK1 inhibition facilitates the "killing" of HIV-infected $CD4^+$ T cells and leads to the reduction of HIV viral reservoirs [15]. Although the antiretroviral therapy is effective to control HIV infection [55], complications associated with KSHV co-infection remain a significant problem. Additionally, there is a clear evidence of poor overall survival of primary effusion lymphoma (PEL) with one study showed that the average survival for HIV-infected PEL patients receiving multi-drug anticancer treatment is 10.2 months [56]. Thus, the regimen of PLK1 and STAT3 inhibitors will be valuable to eliminate KSHV/EBV-infected tumor cells as well viral reservoirs of gamma-herpesviruses (KSHV, EBV) and HIV in these patients.

As summarized in Fig 8C, our studies identified that PLK1 is induced by infection of gamma-herpesviruses (KSHV, EBV) or HIV co-infection, which in return promotes KSHV/EBV viral latency as well as survival of virus-infected tumor cells. PLK1 inhibition destabilizes

c-Myc and reduces histone H3 methylation (H3K27me3) that facilitate both viral reactivation and cell death of KSHV/EBV-reactivated tumor cells. Other PLK1-participating cellular stress and immune signaling pathways may also be involved. Our studies also propose a combinatory regimen of PLK1 and STAT3 inhibitors for efficient reactivation of latent KSHV/EBV as well as induction of cell death of KSHV/EBV-infected tumor cells, leading to significant reduction of KSHV/EBV viral reservoirs. Overall, we have delineated a novel mechanism that depicts interaction between HIV and gamma-herpesvirus in the co-infection scenario, which can be targeted for potential therapeutic use. However, there are several potential limitations of our study. Targeting PLK1 for antiviral and antitumor therapies still needs future evaluation. PLK1 may regulate other host and viral proteins through phosphorylation, which may complicate its function in regulating viral latency and oncogenesis. In certain cancers, Myc protein is upregulated, which may counteract the effect of PLK1 inhibitors. Recently, it has been shown that viral oncolytic approach is promising to treat certain types of cancers. However, viral latency-reversing agents likely need to be combined with other ones to limit viral spreading to other un-infected cells for the viral oncolytic application.

Methods

Cells

Jurkat Clone E6-1 (Cat. # 177) and SLK cells were received from the NIH AIDS reagent program and maintained in RPMI 1640 medium (Invitrogen) supplemented with 10% Fetal Bovine Serum (FBS; Invitrogen). TREx BCBL1-Rta cells [57] were maintained in RPMI 1640 supplemented with 10% FBS, 1% Pen-Strep, 20 mg/ml hygromycin B and 2 mM L-glutamine (Invitrogen). KSHV-positive BCBL1 cells were grown in RPMI 1640 supplemented with 20% heat-inactivated FBS and 2 mM l-glutamine [57]. BJAB cells were maintained in RPMI 1640 medium (Invitrogen) supplemented with 10% fetal bovine serum (FBS; Invitrogen) and 1% Pen-Strep. iSLK.r219 cells [58] were maintained in DMEM medium (Corning) containing 10% FBS, 1% Pen-Strep, 10 μg/ml puromycin (Corning), 250 mg/ml Geneticin (Corning), and 400 mg/ml hygromycin B (Corning). iSLK.BAC16 cells were maintained in the presence of 1 μg/ml puromycin, 250 μg/ml G418, and 1,200 μg/ml hygromycin B [17]. Telomerase-immortalized human microvascular endothelial (TIME) cells were maintained in Vascular Cell Basal Medium (ATCC, cat. # PCS-100-030) supplemented with Microvascular Endothelial Cell Growth Kit-VEGF (ATCC, cat. # PCS-110-041). BC-2 and HBL-6 cells harboring both KSHV and EBV were grown in RPMI 1640 supplemented with 20% and 10% heat-inactivated FBS, respectively. Akata-BX1 cells were maintained in RPMI 1640 supplemented with 10% FBS. EBV-negative Akata cell line was clonally selected for the loss of viral episome from the original EBV-positive Akata Burkitt's Lymphoma cell line, which was subsequently re-infected with EBV BX1 strain and selected with neomycin [59].

Compounds

DMSO was purchased from Fisher Scientific. SBE 13 HCl were purchased from Selleck Chemicals. Recombinant HIV Nef protein (rNef) were provided by NIH AIDS reagent program. The UMB-158 PLK1/BET dual inhibitor was synthesized according to an earlier publication [21] and kindly provided by Wei Zhang (University of Massachusetts at Boston). The STAT3 inhibitors, cryptotansinone and stattic, were purchased from Sigma-Aldrich. 12-O-Tetradecanoylphorbol 13-acetate (TPA, cat. # P8139) and sodium butyrate (NaB, cat. # AAA1107906) were purchased from Sigma-Aldrich and Fisher Scientific, respectively. Doxycycline (Dox) was obtained from Fisher Scientific (Cat. # BP2653-1). Human IgG (Cat. # 55087) were purchased from MP biomedicals.

Viruses

iSLK.BAC16 cells were treated with 1μg/mL Dox and 1mM NaB for 48h. Supernatants were collected 2 dpi, centrifuged (400 × g) for 10 mins to remove cellular debris, and filtered through the 0.45μm filter. The harvested supernatants containing KSHV.BAC16 viruses were incubated with pre-seeded SLK and TIME cells cultured in the 1:1 and 2:1 ratio of fresh media along with 8μg/mL polybrene via spinoculation (2500 rpm) for 2h at 37˚C. HIV-1 IIIB wild-type virus was kindly provided by the NIH AIDS reagent program [60,61]. Jurkat cells were subjected to HIV-1 IIIB infection at multiplicity of infection (MOI) = 1 for 5 days [15,61].

Antibodies

ChIP-grade mouse anti-PLK1 (Cat. # SAB1404220) and mouse IgG (Cat. # sc2025) antibodies were obtained from Sigma Aldrich. Anti-FLAG (Cat. # 2368) antibody was purchased from Cell Signaling Technology. Mouse anti-V5 (Cat. # R960-25), anti-HA (Cat. # 26183), HRP-conjugated goat anti-Mouse IgG (H+L) secondary antibody (Cat. # 31430), HRP-conjugated goat anti-Rabbit IgG (H+L) secondary antibody (Cat. # 31460) were purchased from Thermo Fisher Scientific. Antibodies against c-Myc (Cat. # 9E10: sc-40), HHV-8 K8.1A/B (Cat. # sc-65446), EBV ZEBRA (Cat. # sc-53904), GAPDH (Cat. # sc-32233) were purchased from Santa Cruz Biotechnology. Antibodies against H3K27Me3 (Cat. # 39155), H3K9Me3 (Cat. # 61013) were purchased from Active Motif, and histone H3 antibody (Cat. # 9715S) was purchased from Cell Signaling Technology.

siRNAs and shRNAs

For siRNA knockdown assays, PLK1 siRNA (Cat. # s449) or non-targeting control (NT) siRNA (Cat. # AM4636) was purchased from Thermo Fisher Scientific. TREx BCBL1-Rta and BCBL1 cells were transiently reverse-transfected with siPLK1 (50nM) or siNT (50nM), and SLK cells with siPLK (10nM) or siNT (10nM) using RNAiMAX reagents [62] according to the manufacturer's instruction. Cells were kept in culture for 72 hrs. These cells were treated with Dox (2μg/ml) to induce KSHV reactivation. For shRNA assays, endogenous PLK1 was knocked down in Akata-BX1 cells by using its shRNA expressed from the pINDUCER10 Dox-inducible lentiviral vector, according to the reported protocol [63,15]. Briefly, pINDUCER10 expressing shRNAs (S1 Table) was transiently transfected in Akata-BX1 cells using TurboFect transfection reagent (Thermo fisher scientific) according to the manufactures protocol. Cells were kept in culture for 72 hrs. These cells were treated with Dox to induce shRNA expression and human IgG (2 μg/ml) to induce EBV reactivation for 48 hrs.

Measurement of KSHV/EBV copy number

Cells were either treated with SBE or reverse-transfected with siRNAs for 48h. KSHV/EBV was reactivated by treating cells with TPA/NaB for 48h, followed by the collection of supernatants. Viral DNAs were extracted using the DNeasy Blood & Tissue Kit (Qiagen, cat. # 69504) according to the manufacturer's instruction. Viral copy number was quantified by qPCR using the primers targeting KSHV-LANA and EBV-EBNA1. Plasmids containing the single copy of LANA (pA3M-LANA) or EBNA1 (MSCV-N EBNA1, Addgene, cat. # 37954) were used as the reference.

Isolation of primary B cells

Peripheral blood mononuclear cells (PBMCs) from HIV-infected individuals were acquired from Vitrologic Biological source (Charleston, SC). PBMCs from healthy donors were

purchased from STEMCELL Technologies (Cambridge, MA). PBMCs from HIV+/- donors were subjected to B-cell isolation. Briefly, PBMCs were captured by using an anti-CD19 antibody conjugated to colloidal paramagnetic microbeads (B-cell isolation kit; Miltenyi Biotec, Bergisch-Gladbach, Germany) and passed through a magnetic separation column (LS; Miltenyi Biotec). The purity of isolated B cells was over 95% as assessed by flow cytometry analysis of PE-CD19$^+$ cells (Miltenyi Biotec) [64].

Chromatin immunoprecipitation (ChIP)

ChIP assay was conducted according to the manufacturer protocol (Millipore Sigma, cat. # 17–395) as previously described [65]. Briefly, TREx BCBL1-Rta cells were cross-linked by using 0.5% formaldehyde, followed by treatment with 1 × glycine to quench the reaction. Cells were washed with cold 1 × PBS, and nuclei were isolated using nuclei isolation buffer with rigorous vertexing. Nuclear lysates were sonicated for 2 mins to fragment genomic DNAs. All extraction procedure was carried out in the presence of protease inhibitor cocktail. 1% input were separated before the next step. The lysates were incubated with pre-washed Magna ChIP A/G beads along with specific antibodies or control IgG for overnight at 4˚C. Samples were subjected to subsequent washes and eluted through magnetic separator. Each sample was treated with proteinase K. To reverse the cross-linking, the eluted samples were incubated at 65˚C for 2 hrs and then 95˚C for 15 mins. Next, final magnetic separation was performed to elute the samples. KSHV lytic gene expression was quantified by real-time PCR. Input (1%) was used for qPCR analysis.

Confocal and fluorescence microscopy

For iSLK.r219 cells, fluorescence was measured on a BioTeK plate reader by using its GFP and RFP channels. Expression of GFP and RFP proteins from KSHV.r219 viral strain are respectively driven by the eIF1a promoter and KSHV lytic PAN promoter [66]. SLK and iSLK. BAC16 cells were seeded onto the high precision cover glasses (Bioscience Tools, cat. # CSHP-No1.5–13) pre-coated with poly-L-lysine (R&D Systems, cat. # 3438-100-01) for 45 mins in a 24-well plate. These cells were induced with 1μg/mL Dox for 48 hrs. The KSHV. BAC16 *de novo* infected SLK cells were also collected in coverslips. Cells were rinsed and fixed with 4% paraformaldehyde at room temperature (RT), followed by permeabilization with 0.05% triton-X reagent for 10 mins at RT. Cells were washed with 1 × PBS and incubated with 5% FBS for 1 hr at RT. Cells were further incubated with an anti-mouse PLK1 antibody in 2.5% FBS for overnight in a moist chamber at 4˚C. Cells were washed to remove the primary antibody and incubated with alexa 647-mouse secondary antibody for 1 hr at RT. Cells were stained with Hoechst (Invitrogen) as per manufacturer's guidelines. Coverslips were rinsed and mounted on slides by using ProLong Glass Antifade Mountant (Invitrogen, cat. # P36982). Slides were left to cure in dark for 24 hrs at RT per manufacturer's recommendations. Confocal images were acquired by using the ZEISS LSM 700 Upright laser scanning confocal microscope and ZEN imaging software (ZEISS). PLK1 were imaged via TAMRA channel while GFP is constitutively expressed in cells infected with KSHV BAC16 [17].

Immunofluorescence assay (IFA)

Isolated B cells were isolated from HIV+/- subjects. Portion of isolated B cells was incubated with CD19 antibody (1/200 of stock, Milteny) for 30 mins to determine the purity using BD Accuri C6 Plus with corresponding optical filters. The rest of B cells was washed and fixed with 4% paraformaldehyde at RT for 20 mins. Pelleted cells were washed and permeabilized with saponin-containing 1 × Perm/Wash buffer (BD Biosciences) as described [15]. Cells were

incubated with an anti-PLK1 antibody (200μg/ml) diluted in 1 × Perm/Wash buffer for overnight at 4˚C, followed by incubation with the fluorophore-conjugated secondary antibody for 1 hr at RT in the dark. The staining buffer (1 × D-PBS with 2% bovine serum albumin [BSA]) was added to resuspend the cells, followed by flow cytometry analysis using the BD Accuri C6 Plus with corresponding optical filters. For the Jurkat and BJAB co-culture assays, BJAB cells were labeled separately with CFSE (Thermo Fisher) for 30 mins according to instruction and incubated with HIV-1 IIIB infected Jurkat cells. These cells were incubated with anti-PLK1 antibody, and subsequently the fluorophore-conjugated secondary antibody. The mean fluorescence intensity (MFI) and the percentage of fluorescence-positive cells were determined by using the FlowJo V10 software.

Immunoblotting assay

Immunoblotting was carried out using the existing protocol [15,61]. In brief, cell pellets were homogenized in ice with 1 × RIPA containing protease inhibitor cocktail. The cell lysate was cleared by centrifugation at 12,000 rpm for 10 mins. The protein concentration was measured by BCA kit (Thermo Fisher Scientific). The same amount of protein samples was boiled in 2 × SDS loading buffer, separated by SDS-PAGE, and transferred to PVDF membrane. The blots were blocked with 5% skimmed milk in 1 × PBS and probed with the specific primary antibodies followed by HRP-conjugated secondary antibodies. Protein bands were visualized with ECL Plus chemiluminescence reagent.

Cell viability and death assays

The cytotoxicity of compounds was determined by using the ATP- based CellTiter-Glo Luminescent Cell Viability Assay (Promega) and analyzed by the Cytation 5 multimode reader (luminescent mode). Death of virus-infected or compound-treated cells was determined by using the LIVE/DEAD Fixable Far Red Dead Cell Stain Kit (Invitrogen) and analyzed by the BD Accuri C6 Plus (flow cytometry) [15].

Cell apoptosis assay

The Vybrant Apoptosis Assay Kit (Thermo Fisher, cat. # V13243) was used to measure cell apoptosis. YO-PRO-1 and propidium iodide (PI) nucleic acid staining was performed following the manufactures instructions. YO-PRO-1 selectively passes through the plasma membrane of apoptotic cells and labels them with green fluorescence. Necrotic cells are stained witht the red-fluorescent PI [67].

Real-time qPCR (RT-qPCR)

Extraction of genomic DNA was performed by using the DNeasy Blood & Tissue Kit (Qiagen, cat. # 69504) according to the manufacturer's instruction. Total RNAs were extracted from the assayed cells by using the RNeasy kit (Qiagen), and 0.2–1 μg of RNA was reversely transcribed using the iScript cDNA Synthesis Kit (Bio-Rad). Real-time PCR assay was conducted using the SYBR Premix ExTaq II (Bio-Rad) and gene-specific primers (S1 Table). The PCR reactions were performed on a Bio-Rad CFX connect qPCR machine under the following conditions: 95 ˚C for 10 mins, 40 cycles of 95 ˚C for 15 secs and 60 ˚C for 1 min. Relative percentage of gene expression was normalized to GAPDH control, and was calculated using the formula: $2^{(\Delta C T \text{ of gene} - \Delta CT \text{ of GAPDH})}$.

RNA isolation from paraffin tissue

Paraffin-embedded tissue sections were deparaffinized by using xylene solution twice with each for 5 mins at RT followed by the high-speed centrifugation at 12,000 rpm for 20 mins. Isolated pellets were washed with graded alcohol (100, 90, 70%) and centrifuged at 12,000 rpm for 10 mins. Air-dried pellets were digested with the buffer containing 4M guanidine thiocyanate and 1M Tris-HC1 (pH 7.6) in DEPC-treated water. 0.3% β-mercaptoethanol was added in the digestion buffer in addition to proteinase K (6 mg/mL) for another incubation at 45˚C for overnight. 1 vol of phenol-water/chloroform (70/30) was added and vortexed rigorously. The mixture was kept on ice for 15 mins and centrifuged at 12,000 rpm for 20 mins. The upper aqueous phase was collected by avoiding the proteinaceous interface between the two phases, and transferred to a new test tube. 1 vol of isopropanol was added in addition to 1mg/ml glycogen. The aqueous phase was kept at -80˚C for 2 hrs, followed by the centrifugation at 12,000 rpm for 20 mins at 4˚C. RNA pellets were washed with ethanol (75%) and kept at -20˚C for overnight. RNA pellets were centrifuged at 12,000 rpm for 5 mins and air-dried. DEPC-treated water was added to resuspend the pellet and dissolve the RNA.

Statistical analysis

Statistical analysis was performed in GraphPad PRISM 5 or Excel. Data are presented as mean ± SD of independent experiments (n = 3). * $p<0.05$ and ** $p<0.01$ with two-tailed paired Student t-test except specified otherwise.

Supporting information

S1 Fig. (A) TIME cells were *de novo* infected with KSHV.BAC16 viruses collected from supernatants of Dox-treated iSLK.BAC16 cells. At 48h post-of-infection, GFP+ cells were analyzed by fluroscence imaging or flow cytometry. (B) Cells in (A) were subjected to immunofluorescence assays of PLK1 and analzyed by flow cytometry. Mean fluorescence intensity (MFI) of PLK1 in these cells was measured. Alternatively, cells in (A) were also subjectd to PLK1 protein immunoblotting and mRNA RT-qPCR assays. Results were presented as mean ± SD (* $p<0.05$; two-tailed paired Student t-test). (C) SLK cells were transiently transfected with the indicated siRNAs (siNT, siPLK1-1, siPLK1-2), and subjected to PLK1 protein immunoblotting and cell viability assays. (D) BCBL1 cells were transiently transfected with the indicated siRNAs (siNT, siPLK1-1, siPLK1-2), and analyzed for PLK1 knockdown by RT-qPCR assays. (E) Cells in (D) were treated with TPA/NaB or mock, and supernatants were harvested and analyzed for KSHV viral DNA copy number by qPCR assays using primers targeting ORF73/LANA (KSHV). The standard curve was prepared by using the pA3M-LANA plasmid. The viral DNA copy number was calculated from the standard curve and normalized to cells. Results were presented as mean ± SD (* $p<0.05$; two-tailed paired Student t-test). (F) mRNA level of PLK1 in iSLK.r219 cells transiently transfected with the pLEX-FLAG or pLEX-PLK1 vector was measured by RT-qPCR. (* $p<0.05$; two-tailed paired Student t-test).
(TIF)

S2 Fig. (A) Cell viability of iSLK.r219 cells treated with SBE at the increasing dose as well as Dox was measured by ATP-based assay. (B) BCBL1, BC-2, and HBL-6 cells were treated with SBE in the presence or absence of TPA/NaB, and supernatants were harvested and analyzed for KSHV viral DNA copy number by qPCR assays using primers targeting ORF73/LANA (KSHV). The standard curve was prepared by using the pA3M-LANA plasmid. The viral DNA copy number was calculated from the standard curve and normalized to cells. Results were presented as mean ± SD (* $p<0.05$; two-tailed paired Student t-test). (C) TREx BCBL1-Rta

cells treated with SBE in the presence or absence of Dox was subjected to PLK1 protein immunoblotting assays. (D) mRNA level of KSHV lytic genes (ORF50, K8.1) in iSLK.r219 cells treated with BI-2536 or BI-6727 in the presence or absence of Dox was analyzed by qPCR and normalized to GAPDH. (* $p<0.05$; two-tailed paired Student t-test).
(TIF)

S3 Fig. (A, B) Cell viability of TREx BCBL1-Rta (A) or BCBL (B) cells treated with SBE with or without Dox was measured by ATP-based assay. In parallel, cell viability of KSHV/EBV-negative BJAB cells treated with SBE alone was also measured. (C) Cell viability of TREx BCBL1-Rta cells treated with UMB-158 with or without Dox was measured. (* $p<0.05$, ** $p<0.01$; two-tailed paired Student t-test). (D) Cell viability of TREx BCBL1-Rta cells treated with BI-6727 or BI-2536 in the presence or absence of Dox was measured by ATP-based assay. (* $p<0.05$; two-tailed paired Student t-test). (E, F) TREx BCBL1-Rta cells were treated with SBE (E), UMB-158 (F), or DMSO, and induced with Dox. Percentage of necrotic cells was analyzed by flow cytometry of PI-stained cells using Vybrant Apoptosis Assay Kit (Thermo Fisher),.
(TIF)

S4 Fig. (A) mRNA level of cell-cycle genes, cyclin A and cyclin E, in TREx BCBL1-Rta cells treated with SBE or DMSO in the presence of Dox was measured by RT-qPCR and normalized to GAPDH. (B) TREx BCBL1-Rta cells were treated with SBE or DMSO, and Dox to induce KSHV reactivation. Cell lysates were prepared and subjected to ChIP assay by using antibodies against H3K9me3 or a mouse IgG. Precipitated DNA samples were further analyzed by qPCR by using primers targeting promoter region of KSHV lytic genes (ORF50, ORF59) and OriLyt, and normalized to IgG control. (* $p<0.05$; two-tailed paired Student t-test).
(TIF)

S5 Fig. Protein level of KSHV K8.1 in BCBL1 cells treated with CRYP or stattic in the presence or absence of SBE was measured by immunoblotting. GAPDH was used as a loading control.
(TIF)

S6 Fig. (A, B) Cell viability of Akata-BX1 cells treated with SBE (A) or UMB-158 (B) at the increasing dose with or without hIgG induction was measured by ATP-based assay. (* $p<0.05$, treatment vs control; two-tailed paired Student t-test). (C) BC-2 and HBL-6 cells were treated with SBE in the presence or absence of TPA/NaB, and supernatants were harvested and analyzed for EBV viral DNA copy number by qPCR assays using primers targeting EBNA1 (EBV). The standard curve was prepared by using the MSCV-N EBNA1 plasmid. The viral DNA copy number was calculated from the standard curve and normalized to cells. Results were presented as mean ± SD (* $p<0.05$; two-tailed paired Student t-test). (D) Protein level of EBV ZEBRA in Akata-BX1 cells treated with CRYP or stattic in the presence or absence of SBE was measured by immunoblotting. GAPDH was used as a loading control.
(TIF)

S7 Fig. (A) HIV-1 IIIB infection in Jurkat cells was confirmed by immunoblotting of HIV p24 protein. (B) Cell viability of TREx BCBL1-Rta cells treated with rNef protein in the presence or absence of Dox was measured by ATP-based assay. (C) Protein level of KSHV K8.1 in above cells (B) was measured by immunoblotting.
(TIF)

S8 Fig. A serial dilution of TREx BCBL1-Rta (A) or Akata-BX1 (B) cells within KSHV/EBV-negative BJAB cells was prepared, followed by treatment of SBE alone or DMSO. Copy

number of viral DNA genome was measured by qPCR using primers that target ORF73/LANA (KSHV) or EBNA1 (EBV) respectively, and normalized to GAPDH (* $p<0.05$; two-way ANOVA).
(TIF)

S1 Table. Primers used for qPCR assays in this study.
(PDF)

Acknowledgments

We would like to thank Dr. Prashant Desai for HEK293.r219 cells and Dr. Renfeng Li for Akata-BX1 cells. We would also like to thank Dr. Jae Jung for TREx BCBL1-Rta cells and Dr. SJ Gao for iSLK.r219, iSLK.BAC16 and TIME cells. pA3M-LANA was a gift from Dr. Erle Robertson. UMB-158 compound was kindly provided by Dr. Wei Zhang from University of Massachusetts at Boston.

Author Contributions

Conceptualization: Jian Zhu, Netty G. Santoso.

Data curation: Ayan Biswas, Dawei Zhou.

Formal analysis: Ayan Biswas, Dawei Zhou.

Funding acquisition: Jian Zhu, Netty G. Santoso.

Investigation: Ayan Biswas, Dawei Zhou.

Methodology: Ayan Biswas, Dawei Zhou.

Project administration: Jian Zhu, Netty G. Santoso.

Resources: Jian Zhu, Netty G. Santoso.

Supervision: Jian Zhu.

Validation: Ayan Biswas, Dawei Zhou, Guillaume N. Fiches.

Visualization: Ayan Biswas.

Writing – original draft: Ayan Biswas, Jian Zhu.

Writing – review & editing: Ayan Biswas, Dawei Zhou, Guillaume N. Fiches, Zhenyu Wu, Xuefeng Liu, Qin Ma, Weiqiang Zhao, Jian Zhu, Netty G. Santoso.

References

1. Chang Y, Cesarman E, Pessin MS, Lee F, Culpepper J, Knowles DM, et al. Identification of herpesvirus-like DNA sequences in AIDS-associated Kaposi's sarcoma. Science (80-). 1994. https://doi.org/10.1126/science.7997879 PMID: 7997879
2. Antman K, Chang Y. Kaposi's sarcoma. New England Journal of Medicine. 2000. https://doi.org/10.1056/NEJM200004063421407 PMID: 10749966
3. Ambroziak JA, Blackbourn DJ, Herndier BQ, Glogau RG, Gullett JH, McDonald AR, et al. Herpes-like sequences in HIV-infected and uninfected Kaposi's sarcoma patients. Science. 1995. https://doi.org/10.1126/science.7725108 PMID: 7725108
4. Veettil MV, Bandyopadhyay C, Dutta D, Chandran B. Interaction of KSHV with host cell surface receptors and cell entry. Viruses. 2014. https://doi.org/10.3390/v6104024 PMID: 25341665
5. Boshoff C, Chang Y. Kaposi's sarcoma-associated herpesvirus: A new DNA tumor virus. Annual Review of Medicine. 2001. https://doi.org/10.1146/annurev.med.52.1.453 PMID: 11160789

6. Aneja KK, Yuan Y. Reactivation and lytic replication of Kaposi's sarcoma-associated herpesvirus: An update. Frontiers in Microbiology. 2017. https://doi.org/10.3389/fmicb.2017.00613 PMID: 28473805
7. Trivedi P, Takazawa K, Zompetta C, Cuomo L, Anastasiadou E, Carbone A, et al. Infection of HHV-8+ primary effusion lymphoma cells with a recombinant Epstein-Barr virus leads to restricted EBV latency, altered phenotype, and increased tumorigenicity without affecting TCL1 expression. Blood. 2004. https://doi.org/10.1182/blood-2003-05-1710 PMID: 12969959
8. Goradel NH, Mohajel N, Malekshahi ZV, Jahangiri S, Najafi M, Farhood B, et al. Oncolytic adenovirus: A tool for cancer therapy in combination with other therapeutic approaches. Journal of Cellular Physiology. 2019. https://doi.org/10.1002/jcp.27850 PMID: 30515798
9. Attermann AS, Bjerregaard AM, Saini SK, Grønbæk K, Hadrup SR. Human endogenous retroviruses and their implication for immunotherapeutics of cancer. Annals of Oncology. 2018. https://doi.org/10.1093/annonc/mdy413 PMID: 30239576
10. Zhou F, Shimoda M, Olney L, Lyu Y, Tran K, Jiang G, et al. Oncolytic reactivation of KSHV as a therapeutic approach for primary effusion lymphoma. Mol Cancer Ther. 2017. https://doi.org/10.1158/1535-7163.MCT-17-0041 PMID: 28847988
11. Ma X, Wang L, Huang D, Li Y, Yang D, Li T, et al. Polo-like kinase 1 coordinates biosynthesis during cell cycle progression by directly activating pentose phosphate pathway. Nat Commun. 2017. https://doi.org/10.1038/s41467-017-01647-5 PMID: 29138396
12. Chun G, Bae D, Nickens K, O'Brien TJ, Patierno SR, Ceryak S. Polo-like kinase 1 enhances survival and mutagenesis after genotoxic stress in normal cells through cell cycle checkpoint bypass. Carcinogenesis. 2010. https://doi.org/10.1093/carcin/bgq014 PMID: 20089605
13. Li M, Liu Z, Wang X. Exploration of the Combination of PLK1 Inhibition with Immunotherapy in Cancer Treatment. J Oncol. 2018. https://doi.org/10.1155/2018/3979527 PMID: 30631355
14. Ren Y, Bi C, Zhao X, Lwin T, Wang C, Yuan J, et al. PLK1 stabilizes a MYC-dependent kinase network in aggressive B cell lymphomas. J Clin Invest. 2018. https://doi.org/10.1172/JCI122533 PMID: 30260324
15. Zhou D, Hayashi T, Jean M, Kong W, Fiches G, Biswas A, et al. Inhibition of Polo-like kinase 1 (PLK1) facilitates the elimination of HIV-1 viral reservoirs in CD4+ T cells ex vivo. Sci Adv. 2020. https://doi.org/10.1126/sciadv.aba1941 PMID: 32832623
16. Strebhardt K. Multifaceted polo-like kinases: Drug targets and antitargets for cancer therapy. Nature Reviews Drug Discovery. 2010. https://doi.org/10.1038/nrd3184 PMID: 20671765
17. Brulois KF, Chang H, Lee AS-Y, Ensser A, Wong L-Y, Toth Z, et al. Construction and Manipulation of a New Kaposi's Sarcoma-Associated Herpesvirus Bacterial Artificial Chromosome Clone. J Virol. 2012. https://doi.org/10.1128/JVI.01019-12 PMID: 22740391
18. Keppner S, Proschak E, Kaufmann M, Strebhardt K, Schneider G, Spänkuch B. Biological impact of freezing Plk1 in its inactive conformation in cancer cells. Cell Cycle. 2010. https://doi.org/10.4161/cc.9.4.10644 PMID: 20139717
19. Ciceri P, Müller S, O'Mahony A, Fedorov O, Filippakopoulos P, Hunt JP, et al. Dual kinase-bromodomain inhibitors for rationally designed polypharmacology. Nat Chem Biol. 2014. https://doi.org/10.1038/nchembio.1471 PMID: 24584101
20. Lee KS, Burke TR, Park JE, Bang JK, Lee E. Recent Advances and New Strategies in Targeting Plk1 for Anticancer Therapy. Trends in Pharmacological Sciences. 2015. https://doi.org/10.1016/j.tips.2015.08.013 PMID: 26478211
21. Liu S, Yosief HO, Dai L, Huang H, Dhawan G, Zhang X, et al. Structure-Guided Design and Development of Potent and Selective Dual Bromodomain 4 (BRD4)/Polo-like Kinase 1 (PLK1) Inhibitors. J Med Chem. 2018. https://doi.org/10.1021/acs.jmedchem.8b00765 PMID: 30125504
22. Gohda J, Suzuki K, Liu K, Xie X, Takeuchi H, Inoue JI, et al. BI-2536 and BI-6727, dual Polo-like kinase/bromodomain inhibitors, effectively reactivate latent HIV-1. Sci Rep. 2018. https://doi.org/10.1038/s41598-018-21942-5 PMID: 29476067
23. Zhang Y, Du X, Wang C, Lin D, Ruan X, Feng Y, et al. Reciprocal activation between PLK1 and Stat3 contributes to survival and proliferation of esophageal cancer cells. Gastroenterology. 2012. https://doi.org/10.1053/j.gastro.2011.11.023 PMID: 22108192
24. Oltval ZN, Milliman CL, Korsmeyer SJ. Bcl-2 heterodimerizes in vivo with a conserved homolog, Bax, that accelerates programed cell death. Cell. 1993. https://doi.org/10.1016/0092-8674(93)90509-O
25. Kang MH, Reynolds CP. Bcl-2 Inhibitors: Targeting mitochondrial apoptotic pathways in cancer therapy. Clin Cancer Res. 2009. https://doi.org/10.1158/1078-0432.CCR-08-0144 PMID: 19228717
26. Dang C V., Kim JW, Gao P, Yustein J. The interplay between MYC and HIF in cancer. Nature Reviews Cancer. 2008. https://doi.org/10.1038/nrc2274 PMID: 18046334

27. Xiao D, Yue M, Su H, Ren P, Jiang J, Li F, et al. Polo-like Kinase-1 Regulates Myc Stabilization and Activates a Feedforward Circuit Promoting Tumor Cell Survival. Mol Cell. 2016. https://doi.org/10.1016/j.molcel.2016.09.016 PMID: 27773673

28. Li X, Chen S, Feng J, Deng H, Sun R. Myc Is Required for the Maintenance of Kaposi's Sarcoma-Associated Herpesvirus Latency. J Virol. 2010. https://doi.org/10.1128/JVI.00244-10 PMID: 20573831

29. Martinato F, Cesaroni M, Amati B, Guccione E. Analysis of myc-induced histone modifications on target chromatin. PLoS One. 2008. https://doi.org/10.1371/journal.pone.0003650 PMID: 18985155

30. Toth Z, Maglinte DT, Lee SH, Lee HR, Wong LY, Brulois KF, et al. Epigenetic analysis of KSHV latent and lytic genomes. PLoS Pathog. 2010. https://doi.org/10.1371/journal.ppat.1001013 PMID: 20661424

31. King CA, Li X, Barbachano-Guerrero A, Bhaduri-McIntosh S. STAT3 Regulates Lytic Activation of Kaposi's Sarcoma-Associated Herpesvirus. J Virol. 2015. https://doi.org/10.1128/JVI.02008-15 PMID: 26339061

32. Huynh J, Chand A, Gough D, Ernst M. Therapeutically exploiting STAT3 activity in cancer—using tissue repair as a road map. Nature Reviews Cancer. 2019. https://doi.org/10.1038/s41568-018-0090-8 PMID: 30578415

33. Rivera-Soto R, Dissinger NJ, Damania B. Kaposi's Sarcoma-Associated Herpesvirus Viral Interleukin-6 Signaling Upregulates Integrin β3 Levels and Is Dependent on STAT3. J Virol. 2019. https://doi.org/10.1128/jvi.01384-19 PMID: 31801855

34. Ramalingam D, Ziegelbauer JM. Viral microRNAs Target a Gene Network, Inhibit STAT Activation, and Suppress Interferon Responses. Sci Rep. 2017. https://doi.org/10.1038/srep40813 PMID: 28102325

35. Damania B, Münz C. Immunodeficiencies that predispose to pathologies by human oncogenic γ-herpesviruses. FEMS Microbiology Reviews. 2019. https://doi.org/10.1093/femsre/fuy044 PMID: 30649299

36. Minhas V, Crabtree KL, Chao A, M'soka TJ, Kankasa C, Bulterys M, et al. Early childhood infection by human herpesvirus 8 in Zambia and the role of human immunodeficiency virus type 1 coinfection in a highly endemic area. Am J Epidemiol. 2008. https://doi.org/10.1093/aje/kwn125 PMID: 18515794

37. Grogg KL, Miller RF, Dogan A. HIV infection and lymphoma. Journal of Clinical Pathology. 2007. https://doi.org/10.1136/jcp.2007.051953 PMID: 18042692

38. Lenassi M, Cagney G, Liao M, Vaupotič T, Bartholomeeusen K, Cheng Y, et al. HIV Nef is secreted in exosomes and triggers apoptosis in bystander CD4+ T cells. Traffic. 2010. https://doi.org/10.1111/j.1600-0854.2009.01006.x PMID: 19912576

39. Ferdin J, Goričar K, Dolžan V, Plemenitaš A, Martin JN, Peterlin BM, et al. Viral protein Nef is detected in plasma of half of HIV-infected adults with undetectable plasma HIV RNA. PLoS One. 2018. https://doi.org/10.1371/journal.pone.0191613 PMID: 29364927

40. Raymond AD, Campbell-Sims TC, Khan M, Lang M, Huang MB, Bond VC, et al. HIV type 1 Nef is released from infected cells in CD45+ microvesicles and is present in the plasma of HIV-infected individuals. AIDS Res Hum Retroviruses. 2011. https://doi.org/10.1089/aid.2009.0170 PMID: 20964480

41. Homann S, Tibroni N, Baumann I, Sertel S, Keppler OT, Fackler OT. Determinants in HIV-1 Nef for enhancement of virus replication and depletion of CD4+ T lymphocytes in human lymphoid tissue ex vivo. Retrovirology. 2009. https://doi.org/10.1186/1742-4690-6-6 PMID: 19146681

42. Yan Q, Ma X, Shen C, Cao X, Feng N, Qin D, et al. Inhibition of Kaposi's Sarcoma-Associated Herpesvirus Lytic Replication by HIV-1 Nef and Cellular MicroRNA hsa-miR-1258. J Virol. 2014. https://doi.org/10.1128/JVI.00025-14 PMID: 24554664

43. Bhatt AP, Damania B. AKTivation of PI3K/AKT/mTOR signaling pathway by KSHV. Front Immunol. 2012. https://doi.org/10.3389/fimmu.2012.00401 PMID: 23316192

44. Linnemann T, Zheng YH, Mandic R, Peterlin BM. Interaction between Nef and phosphatidylinositol-3-kinase leads to activation of p21-activated kinase and increased production of HIV. Virology. 2002. https://doi.org/10.1006/viro.2002.1365 PMID: 12009866

45. Boulanger E, Gérard L, Gabarre J, Molina JM, Rapp C, Abino JF, et al. Prognostic factors and outcome of human herpesvirus 8-associated primary effusion lymphoma in patients with AIDS. J Clin Oncol. 2005. https://doi.org/10.1200/JCO.2005.07.084 PMID: 15994147

46. Liu XQ, Cohen JI. The role of PI3K/Akt in human herpesvirus infection: From the bench to the bedside. Virology. 2015. https://doi.org/10.1016/j.virol.2015.02.040 PMID: 25798530

47. Finger LR, Harvey RC, Moore RCA, Showe LC, Croce CM. A common mechanism of chromosomal translocation in T- and B-cell neoplasia. Science (80-). 1986. https://doi.org/10.1126/science.3490692 PMID: 3490692

48. Guo R, Jiang C, Zhang Y, Govande A, Trudeau SJ, Chen F, et al. MYC Controls the Epstein-Barr Virus Lytic Switch. Mol Cell. 2020. https://doi.org/10.1016/j.molcel.2020.03.025 PMID: 32315601

49. Murga-Zamalloa C, Polk A, Hanel W, Chowdhury P, Brown N, Hristov AC, et al. Polo-like-kinase 1 (PLK-1) and c-myc inhibition with the dual kinase-bromodomain inhibitor volasertib in aggressive lymphomas. Oncotarget. 2017. https://doi.org/10.18632/oncotarget.22967 PMID: 29383095

50. Tu WB, Shiah YJ, Lourenco C, Mullen PJ, Dingar D, Redel C, et al. MYC Interacts with the G9a Histone Methyltransferase to Drive Transcriptional Repression and Tumorigenesis. Cancer Cell. 2018. https://doi.org/10.1016/j.ccell.2018.09.001 PMID: 30300580

51. Hopcraft SE, Pattenden SG, James LI, Frye S, Dittmer DP, Damania B. Chromatin remodeling controls Kaposi's sarcoma-associated herpesvirus reactivation from latency. PLoS Pathog. 2018. https://doi.org/10.1371/journal.ppat.1007267 PMID: 30212584

52. García-Gutiérrez L, Delgado MD, León J. Myc oncogene contributions to release of cell cycle brakes. Genes. 2019. https://doi.org/10.3390/genes10030244 PMID: 30909496

53. King CA. Kaposi's Sarcoma-Associated Herpesvirus Kaposin B Induces Unique Monophosphorylation of STAT3 at Serine 727 and MK2-Mediated Inactivation of the STAT3 Transcriptional Repressor TRIM28. J Virol. 2013. https://doi.org/10.1128/JVI.02976-12 PMID: 23740979

54. Beebe JD, Liu JY, Zhang JT. Two decades of research in discovery of anticancer drugs targeting STAT3, how close are we? Pharmacology and Therapeutics. 2018. https://doi.org/10.1016/j.pharmthera.2018.06.006 PMID: 29933035

55. Maskew M, Macphail AP, Whitby D, Egger M, Fox MP. Kaposi sarcoma-associated herpes virus and response to antiretroviral therapy: A prospective study of HIV-infected adults. J Acquir Immune Defic Syndr. 2013. https://doi.org/10.1097/QAI.0b013e3182969cc1 PMID: 23614996

56. Guillet S, Gérard L, Meignin V, Agbalika F, Cuccini W, Denis B, et al. Classic and extracavitary primary effusion lymphoma in 51 HIV-infected patients from a single institution. Am J Hematol. 2016. https://doi.org/10.1002/ajh.24251 PMID: 26799611

57. Nakamura H, Lu M, Gwack Y, Souvlis J, Zeichner SL, Jung JU. Global Changes in Kaposi's Sarcoma-Associated Virus Gene Expression Patterns following Expression of a Tetracycline-Inducible Rta Transactivator. J Virol. 2003. https://doi.org/10.1128/jvi.77.7.4205-4220.2003 PMID: 12634378

58. Myoung J, Ganem D. Generation of a doxycycline-inducible KSHV producer cell line of endothelial origin: Maintenance of tight latency with efficient reactivation upon induction. J Virol Methods. 2011. https://doi.org/10.1016/j.jviromet.2011.03.012 PMID: 21419799

59. Fiches GN, Zhou D, Kong W, Biswas A, Ahmed EH, Baiocchi RA, et al. Profiling of immune related genes silenced in EBV-positive gastric carcinoma identified novel restriction factors of human gammaherpesviruses. PLoS Pathog. 2020. https://doi.org/10.1371/journal.ppat.1008778 PMID: 32841292

60. Beaumont T, van Nuenen A, Broersen S, Blattner WA, Lukashov V V., Schuitemaker H. Reversal of Human Immunodeficiency Virus Type 1 IIIB to a Neutralization-Resistant Phenotype in an Accidentally Infected Laboratory Worker with a Progressive Clinical Course. J Virol. 2001.

61. Kong W, Biswas A, Zhou D, Fiches G, Fujinaga K, Santoso N, et al. Nucleolar protein NOP2/NSUN1 suppresses HIV-1 transcription and promotes viral latency by competing with Tat for TAR binding and methylation. PLoS Pathog. 2020. https://doi.org/10.1371/journal.ppat.1008430 PMID: 32176734

62. Dillon PJ, Gregory SM, Tamburro K, Sanders MK, Johnson GL, Raab-Traub N, et al. Tousled-like kinases modulate reactivation of gammaherpesviruses from latency. Cell Host Microbe. 2013. https://doi.org/10.1016/j.chom.2012.12.005 PMID: 23414760

63. Meerbrey KL, Hu G, Kessler JD, Roarty K, Li MZ, Fang JE, et al. The pINDUCER lentiviral toolkit for inducible RNA interference in vitro and in vivo. Proc Natl Acad Sci U S A. 2011. https://doi.org/10.1073/pnas.1019736108 PMID: 21307310

64. Poeck H, Wagner M, Battiany J, Rothenfusser S, Wellisch D, Hornung V, et al. Plasmacytoid dendritic cells, antigen, and CpG-C license human B cells for plasma cell differentiation and immunoglobulin production in the absence of T-cell help. Blood. 2004. https://doi.org/10.1182/blood-2003-08-2972 PMID: 15070685

65. Ho KH, Chang CK, Chen PH, Wang YJ, Chang WC, Chen KC. miR-4725-3p targeting stromal interacting molecule 1 signaling is involved in xanthohumol inhibition of glioma cell invasion. J Neurochem. 2018. https://doi.org/10.1111/jnc.14459 PMID: 29747239

66. Vieira J, O'Hearn PM. Use of the red fluorescent protein as a marker of Kaposi's sarcoma-associated herpesvirus lytic gene expression. Virology. 2004. https://doi.org/10.1016/j.virol.2004.03.049 PMID: 15246263

67. Michałowicz J, Sicińska P. Chlorophenols and chlorocatechols induce apoptosis in human lymphocytes (in vitro). Toxicol Lett. 2009. https://doi.org/10.1016/j.toxlet.2009.09.010 PMID: 19766705